

Progress and potential for symmetrical solid oxide electrolysis cells

Yunfeng Tian,¹ Nalluri Abhishek,² Caichen Yang,² Rui Yang,² Choi Sihyuk,³

Bo Chi,^{2*} Jian Pu,² Yihan Ling,^{1*} John T.S. Irvine,⁴ and Guntae Kim^{5*}

1. Jiangsu Key Laboratory of Coal-Based Greenhouse Gas Control and Utilization, School of Materials Science and Physics, China University of Mining and Technology, Xuzhou, 221116, China.
2. Center for Fuel Cell Innovation, School of Materials Science and Engineering, Huazhong University of Science and Technology, Wuhan 430074, China.
3. Department of Aeronautics, Mechanical and Electronic Convergence Engineering, Kumoh National Institute of Technology, Gyeongbuk 39177, Republic of Korea.
4. School of Chemistry, University of St Andrews, St Andrews, Fife, KY16 9ST Scotland, UK.
5. School of Energy and Chemical Engineering, Ulsan National Institute of Science and Technology (UNIST), Ulsan 44919, Republic of Korea.

* Corresponding author.

Email: lyhyy@cumt.edu.cn (Yihan Ling) chibo@hust.edu.cn (Bo Chi)

[gkim@unist.ac.kr](mailto:gtkim@unist.ac.kr) (Guntae Kim)

SUMMARY: Recently, symmetrical solid oxide electrolysis cells (SSOECs) with the same electrode materials as both the anode and cathode have attracted lots of attention, because of their simple manufacturing process and low cost. Moreover, it can narrow the trouble of chemical incompatibility, thermal mismatching, and also these SSOECs are more convenient in practical application without distinction of cathode and anode. However, there is no comprehensive and critical review to summarize the recent progress of SSOECs so far. In this paper, their development history, fundamental mechanisms, electrolyte and electrode materials, and fabrication methods are highlighted. Fuel-assisted SSOECs to decrease the over potential and other applications based on SSOECs are introduced. Furthermore, the challenges and prospects for future research into SSOECs are included, to some extent, offering critical insights and useful guidelines for knowledge-based rational design of better electrodes for commercially viable SSOECs.

KEYWORDS: Symmetrical solid oxide electrolysis cells; Electrolyte materials; Electrode materials; Fabrication methods; Outlook.

Progress and potential

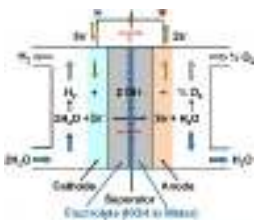
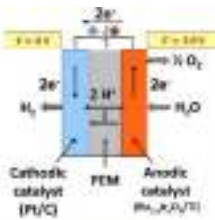
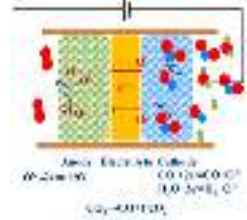
Electrolysis is the core technology of power-to-X solutions, where X can be hydrogen, syngas, or synthetic fuels. Solid oxide electrolysis cells have received growing attention because of unrivaled conversion efficiencies—a result of favorable thermodynamics and kinetics at higher operating temperatures. Symmetrical solid oxide electrolysis cells with the same electrode materials as both the anode and cathode have attracted lots of

attention, because of their simple manufacturing process and low cost. However, there has not been a comprehensive and critical review to summarize the recent progress of them so far. This review is timely, since it gives a comprehensive overview of their development history, fundamental mechanisms, electrolyte and electrode materials, fabrication methods and potential applications. In the end, we share our perspectives on the remaining challenges and potential solutions for driving this emerging field forward. This review will provide food for thought to researchers in the field and a jump-start to beginners who want to join this exciting field.

INTRODUCTION

With the rapid development of social economy, the demand for energy of human beings is further increased. Nowadays, energy consumption and environmental pollution caused by traditional fossil energy-based energy systems have resulted in a series of serious problems in human life.¹⁻³ Therefore, using clean and renewable energy has grown up to be a common goal throughout the world. Many countries have set targets and strategies to achieve 100% use of green and renewable energy by 2050.⁴⁻⁶ Renewable energy sources such as wind energy and solar energy are now widely used and will become the main energy sources in the future. However, a key feature of these renewable energy sources is intermittent supply. Wind energy depends on climatic conditions, sunlight and tides have cycles throughout the day. To overcome these drawbacks, energy conversion and storage technologies are urgently required.⁷⁻¹⁵ Among them, electrolytic cell technology has received more attention due to their high efficiency, environmental friendliness and wide applications.¹⁵⁻¹⁹ Different types of electrolysis cell were developed based on this concept so far, including alkaline electrolysis cell (AEC),²⁰⁻²² polymer electrolyte membrane electrolysis cell (PEMEC)^[23-25] and solid oxide electrolysis cell (SOEC)²⁶⁻²⁸. These three types of electrolysis cell have been systematically compared as displayed in **Table 1**. It can be seen that SOEC is the most effective way due to their low cost and high efficiency.

Table 1. Comparison of three types of electrolysis cells.

			
	Alkaline electrolysis cell (AEC)	Polymer electrolyte membrane electrolysis cell (PEMEC)	Solid oxide electrolysis cell (SOEC)
Temperature	< 100 °C	< 150 °C	> 500 °C
Electrolyte	Liquid solution	Polymer	Ceramic
Cathode	Metal	Metal	Perovskite
Anode	Pt	Ir/Pt	Cermet /perovskite
Charge Carrier	OH ⁻	H ⁺	O ²⁻ /H ⁺
Advantage	Rich products High faradaic efficiency	Rich products High current density High faradaic efficiency	High current density High faradaic efficiency Good stability High energy efficiency
Disadvantage	Low current density Poor energy efficiency Insufficient stability	Poor energy efficiency Insufficient stability	Simple products Chemical incompatibility under high temperature

SOEC can cleanly and efficiently convert the redundant renewable energy (solar, wind and tidal energy) into chemical energy, which plays a vital role in peak-fill of the power grid especially under the background of vigorously developing renewable energy. This is in order to solve the energy crisis and environmental pollution caused by the massive use of fossil energy. SOEC is a very promising technology for converting a variety of renewable electrical energy and heat energy into chemical energy as shown in Figure.1.²⁹⁻³⁰ At the same time, it can use waste heat from the factory to improve energy efficiency. The requirement of electric energy would decrease with the

increasing operation temperature.^{29,31} SOEC can electrolyze H₂O to produce hydrogen, CO₂ electrolysis for reducing the CO₂ emission, and co-electrolyze H₂O/CO₂ to produce syngas (H₂/CO) for chemical production. It has numerous advantages: high efficiency, environmental friendliness, wide-range in application, high electrolysis current, modular design and high reliability. Therefore, SOEC has attracted more and more attention due to its huge development potential.³²⁻³⁵



Figure 1. Schematic diagram of energy conversion and storage based on solid oxide electrolysis cells technology.

Theoretically, SOEC is the reverse process of solid oxide fuel cell (SOFC), so it inherits the development of SOFC.³⁶⁻³⁷ The traditional SOECs have a “sandwich” structure with a dense electrolyte in the middle and porous cathode and anode layers on both sides. Generally, the anode and the cathode are composed of different materials.

For example, the most traditional Ni- $\text{Y}_{0.08}\text{Zr}_{0.92}\text{O}_{2-\delta}$ (YSZ)/YSZ/ $\text{La}_{0.8}\text{Sr}_{0.2}\text{MnO}_{3-\delta}$ (LSM) configuration cell can be described as A/B/C structure, which is asymmetrical configuration with difference materials named as traditional SOEC.³⁸⁻⁴⁰ For the preparation of SOEC, it is usually necessary to prepare a support by tape casting or dry-pressing, and then prepare a cathode and an anode by screen printing. In addition, its sintering process is also more complicated. The first step is to sinter the support, then another sintering process for each electrode is sequentially required. It has complex fabrication process because at least two thermal steps are required for the fabrication of asymmetrical cell. More thermal steps in production mean more energy consumption. Moreover, asymmetric cells also have the following disadvantages: high fabrication cost, two kinds of electrode-electrolyte interfaces, thermal mismatching with the electrolyte as shown in **Figure. 2(A)**.

The chemical incompatibility and thermal mismatching of electrode-electrolyte can be effectively solved if the same material is applied to both electrodes, named symmetrical solid oxide electrolysis cell (SSOECs).⁴¹ They are A/B/A type structure and have great advantages over conventional SOECs as shown in **Figure. 2(B)**. Compared with an asymmetric SOEC, there is only one electrode material. Therefore, the screen printing step will become simple, and the sintering of the electrode can also be completed in a single thermal treatment. It can reduce the fabrication process and cost. Moreover, it can alleviate the trouble of chemical incompatibility, thermal mismatching, and also these SSOECs are more convenient in practical application without distinction of cathode and anode. In fact, a real advantage of SSOECs is that it

can reduce the complexity of electrolyte/electrode interface, which makes it easier to clarify reaction mechanism. Minfang Han et al used a systematical and practical approach to identify the rate-limiting elementary reactions of the redox-stable electrodes in symmetrical SOFCs. ⁴²

Although SSOECs have these glorious advantages, compared to traditional SOECs, the accompanying challenge is that the electrode of SSOECs must both exhibit high electro catalytic activity and good stability towards oxygen evolution reaction (OER), CO₂ or H₂O reduction reaction (CO₂-RR or HER). The electrode material needs to have a thermal expansion coefficient matching the electrolyte. Moreover, it needs to have appropriate chemical compatibility, electrical conductivity and stability in the test environment, which puts higher requirements on the choice of electrodes.

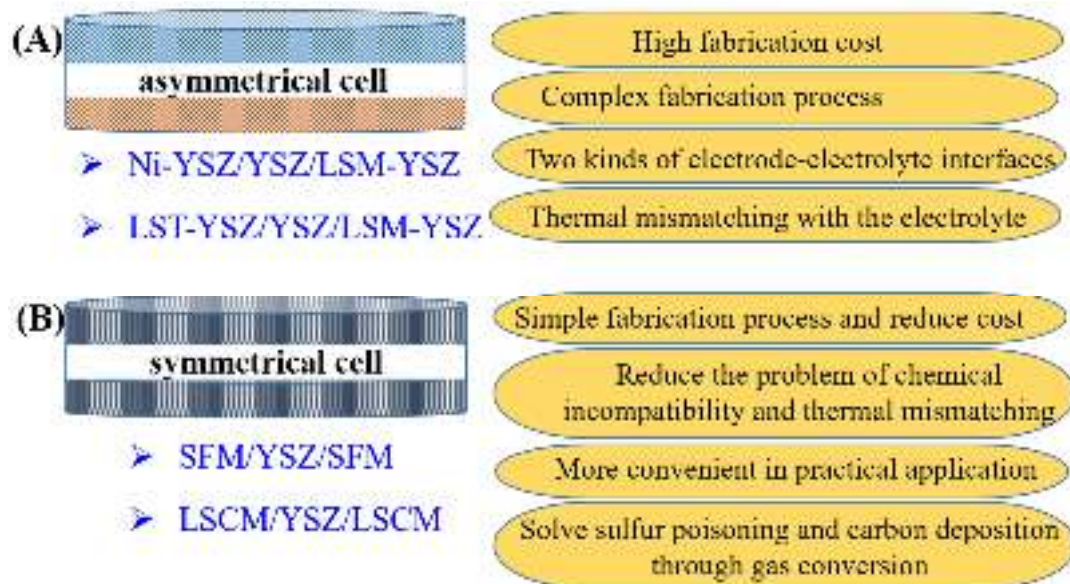


Figure 2. The comparison of asymmetrical cell (A) and symmetrical cell (B).

Fanglin Chen et al. proposed symmetrical SOEC in 2010. ¹⁹ Perovskite oxide Sr₂Fe_{1.5}Mo_{0.5}O_{6-δ} (SFM) has been successfully synthesized and employed as both anode and cathode in SOECs for H₂O electrolysis. From then on, the research for SSOECs

emerged. Many materials as the electrode of SSOEC have been developed for H₂O and CO₂ electrolysis, and some are also used for H₂O-CO₂ co-electrolysis. The structural stability of the electrode material and the catalytic activity in the corresponding atmosphere are the focus of attention. The electrochemical performance of SSOEC has been continuously improved with the development of materials and structural improvements. However, the H₂O or CO₂ electrolysis mechanism of SSOEC is still rarely studied. In addition, new application potentials of SSOEC still need to be tapped. To date, there is lack of a comprehensive and critical review to summarize the recent progress of SSOECs. The developments suggest that a review articulating the differences in the various SSOECs in the literature is due and kept very helpful for understanding SSOECs as well as providing useful guidelines for further development. Herein, we will summarize recent progress on developing electrodes for SSOECs, discussing their development history and fundamental mechanisms. We are then spotlight examples where fuel-assisted SSOECs to decrease the over potential and other applications based on SSOECs, to some extent, providing critical insights and useful guidelines for knowledge-based rational design of better electrodes for commercially viable SSOECs.

RECENT DEVELOPMENTS IN SSOECs

Fundamentals of SSOECs

As the reverse process of SOFC, the first use of SOEC was to produce O₂ with electrolysis CO₂ on Mars in NASA's Mars missions in 1969.⁴³ In the 1980s, Isenberg proposed the use of SOEC as a means of energy conversion for the H₂O/CO₂

electrolysis to produce H_2/CO and O_2 .⁴⁴ After that, SOEC technology has been paid more and more attention due to the increasingly prominent energy crisis and environmental problems.^{1,45} Badding et al. first proposed symmetrical SOFC in 2001,⁴⁶ From then on, the research for SSOFCs emerged.⁴⁷⁻⁵² In 2010, Fanglin Chen et al. investigated a novel electrode material ($Sr_2Fe_{1.5}Mo_{0.5}O_{6-\delta}$) with high electrical conductivity in both air and hydrogen environments, excellent redox stability, and promising performance as electrodes in symmetrical SOFCs. The cell achieves peak power density over $835\text{ mW}\cdot\text{cm}^{-2}$ and $230\text{ mW}\cdot\text{cm}^{-2}$ at $900\text{ }^\circ\text{C}$ using H_2 and wet CH_4 as fuel, respectively.⁵³ In the same year, this material was also used as an electrode for symmetrical SOEC to electrolysis of H_2O . This is the first time report about SSOEC.¹⁹ According to the different types of electrolytes, SSOEC can be divided into the following two categories: oxygen ion conductive symmetrical electrolytic cell (O-SOEC) and proton conductive symmetrical electrolytic cell (H-SOEC). The working principle of the SSOEC has mentioned above in **Figure. 3**. The electrolyte is utilized for transporting oxygen ions (i.e., oxygen ion-conducting O-SOEC) or protons (i.e., proton-conducting H-SOEC) and it should have good ion migration ability. The corresponding basic working principles of two types of cells are illustrated in **Figure. 3 (A) and (B)**, respectively. Specifically, for the O-SOEC, H_2O molecules at the cathode obtain electrons under the effect of an applied voltage, generating H_2 and O^{2-} . O^{2-} anions are driven by the applied electric field from the cathode through the dense electrolyte to the anode. Then O_2 molecules are produced and electrons are released. For the H-SOEC, H_2O molecules at the anode lose electrons under the effect of the

applied voltage, generating H^+ and O_2 . H^+ cations are driven by the applied electric field from the anode through the dense electrolyte to the cathode, generating H_2 .⁵⁴⁻⁵⁶

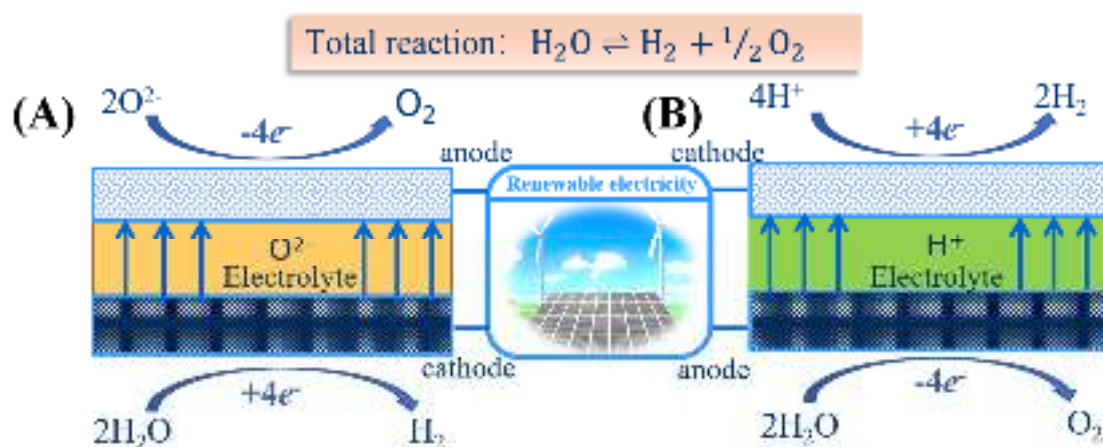


Figure 3. The working principles of oxygen ion-conducting O-SOEC (A) and proton-conducting H-SOEC (B).

SSOEC's unique all-solid-state device characteristics make it ideal for operation in the high temperature range of 700-1000 °C. On one hand, high temperature operation is conducive to the electrode reaction kinetics process, because higher temperature will accelerate the electrode reaction kinetics and reduce the cell resistance, thus improving the performance of SSOEC. On the other hand, high temperature operation can reduce the demand for electrical energy. The thermal energy provided by high temperature operation occupies a large part of the total energy required for electrolysis, especially when using some high-quality thermal energy, such as nuclear reactor thermal energy, geothermal energy, etc. The total energy demand (ΔH) of high-temperature SOEC consists of electrical energy demand (ΔG) and thermal energy demand ($T\Delta S$), as shown in Eq (1):

$$\Delta H = \Delta G + T\Delta S \quad (1)$$

The relationship between the energy required for high temperature H₂O and CO₂ electrolysis and the operating temperature is displayed in **Figure 4**.⁵⁷ As the temperature increases, the heat energy provided increases, and the electrical energy demanded by SOEC gradually decreases. Especially for the CO₂ electrolysis, the trend of increasing the temperature is more noticeable for reducing demand for electric energy. Because the anode and cathode use the same material, the structure of SSOEC is very simple. Therefore, the key materials of SOEC are electrodes and electrolytes.

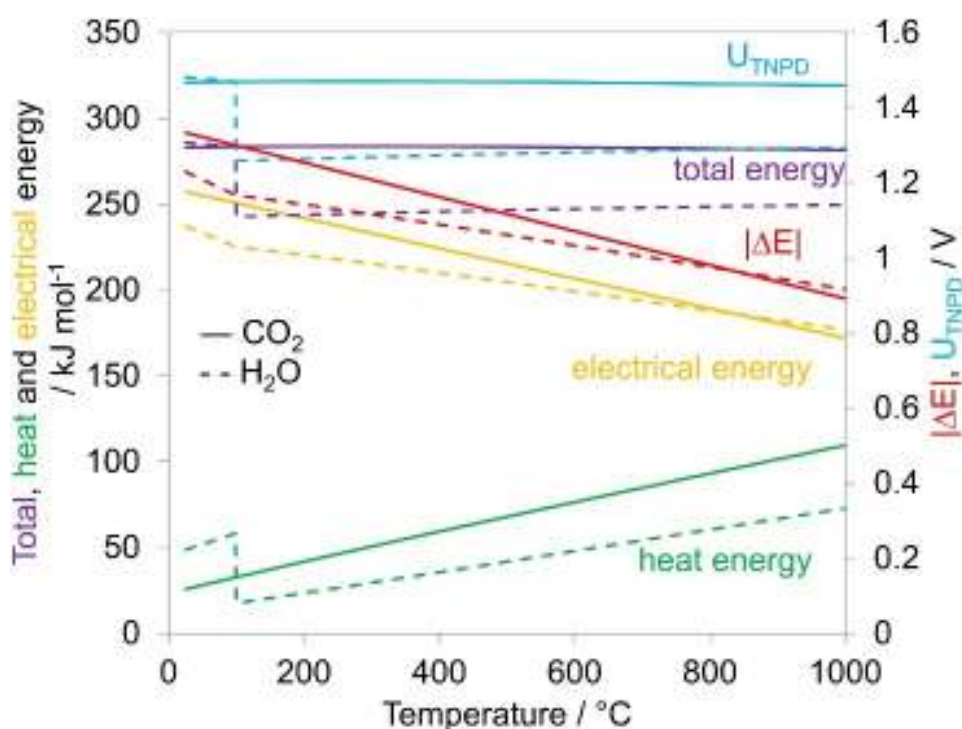


Figure 4. Thermodynamic diagram of H₂O and CO₂ electrolysis.⁵⁷ Copyright 2015, The ELSEVIER.

Electrolyte

The main function of the SSOECs electrolyte is to transport ion between the two electrodes and to isolate the fuel gas and the oxidizing gas. It is one of the core components in the components of the SSOEC. The electrolysis performance of the

electrolysis cell is closely associated with density and conductivity of electrolyte materials. According to the difference of electrolyte conductive ion types, there are two categories of electrolytes are more commonly used, namely oxygen ion conductive (O-SOEC) and proton conductive (H-SOEC).

Oxygen ion conductive electrolyte

For oxygen ion conductive electrolyte materials, they are usually necessary to meet the following conditions:⁵⁸

- a. High oxygen ion conductivity and negligible electronic conductivity;
- b. Good thermal stability and chemical stability. Specifically, it can maintain chemical, structural and dimensional stability under the oxidizing and reducing atmosphere. It also does not react with the electrode material;
- c. High enough density to avoid gas leakage;
- d. Low cost and easy to process.

At present, commonly used oxygen ions electrolyte materials for O-SSOEC mainly include yttrium-stabilized zirconia (YSZ),⁵⁹ scandium-stabilized zirconia (SSZ),⁶⁰ strontium and magnesium doped lanthanum gallium ($\text{La}_{0.9}\text{Sr}_{0.1}\text{Ga}_{0.8}\text{Mg}_{0.2}\text{O}_3$, LSGM).⁵³ YSZ is the most commonly used and lowest cost electrolyte material due to its suitable conductivity and mechanical properties at high temperature. However, its compatibility with electrode material containing La or Sr element is weak which is easy to react with perovskite material and generate high resistance phases $\text{La}_2\text{Zr}_2\text{O}_7$ or SrZrO_3 .⁶¹⁻⁶² The conductivity of YSZ at medium temperature (600 °C -800 °C) is only $0.003 \text{ S}\cdot\text{cm}^{-1}\sim 0.03 \text{ S}\cdot\text{cm}^{-1}$, which limits its development at medium and low

temperature.⁶³ Minimum operating temperature of YSZ is about 700 °C. SSZ achieved higher ionic conductivity than YSZ. At 1000 °C, the ionic conductivity of SSZ is 3 times higher than that of YSZ, so it can be used at moderate temperatures.⁶⁴ However, the abundance of Sc element and its high price prevents its further promotion. Though CeO₂-based electrolyte has a high conductivity at intermediate and low temperature, but Ce⁴⁺ will be reduced to Ce³⁺ in reduction atmosphere, resulting in partial electronic conductance decaying in the cell, which eventually leads to low Faraday efficiency.⁶⁵⁻⁶⁶ Therefore, CeO₂-based electrolytes have almost no application in the field of SOEC. Taking into account the quality of the mixed conductors of these materials under intermediate temperature conditions, they are often added to the electrode materials to improve the electrochemical performance of the electrode materials. LSGM is currently the most concerned intermediate temperature electrolyte material. Compared with YSZ, it has a higher ionic conductivity, which can reach 0.17 S·cm⁻¹ at 800 °C.⁵⁸ However, it has some defects such as difficulty processing and proneness to the second phase LaSrGaO₄ in the preparation process.⁶⁷

Proton conductive electrolyte

For H-SSOEC, on account of the higher ion conductivity and lower activation energy of proton conductors at low temperature range (400 to 700 °C),⁶⁸⁻⁶⁹ therefore, the operation temperature of H-SOECs can be lower than O-SOECs. In fact, reducing the operation temperature of SOECs can broaden the selection range of sealing and connection materials.

Iwahara et al. found that zirconates (zirconia, Zr) and alkaline earth cerates

(cerium, Ce) such as barium cerium oxide (BaCeO_3), strontium zirconium oxide (SrZrO_3) and strontium cerium oxide (SrCeO_3) possessed high protonic conductivity in hydrogen environment at high temperatures in the early 1980s.⁷⁰ Up to now, there are four main groups of perovskite-structured oxides used for H-SOEC, including simple perovskite structure proton conductor (cerium-based perovskite structure electrolyte, Zr-based perovskite structure electrolyte), single-doped zirconate–cerate-based proton conductor ($\text{BaCe}_x\text{Zr}_{1-x}\text{O}_3$ -based electrolyte), composite perovskite structure electrolyte and hybrid-doped zirconate–cerate-based proton conductor. Among them, $\text{Ba}(\text{Zr}_{0.1}\text{Ce}_{0.7}\text{Y}_{0.2})\text{O}_3$ (BZCY),⁷¹ $\text{BaCe}_{0.5}\text{Zr}_{0.3}\text{Y}_{0.16}\text{Zn}_{0.04}\text{O}_{3-\delta}$ (BCZYZ)⁷² etc exhibit excellent and high proton conductivity. However, these oxides still face challenges in a H_2O or CO_2 containing atmosphere at typical operating temperature. Recently, a hybrid ion conductor $\text{BaZr}_{0.1}\text{Ce}_{0.7}\text{Y}_{0.2-x}\text{Yb}_x\text{O}_{3-\delta}$ have been recognized suitable for H-SOEC due to their high conductivity and stability towards H_2O and CO_2 .⁷³⁻⁷⁵ Current research work is mainly focused on improving cell performance and exploring new proton conductor materials. However, there is still a large gap between the overall performance of the cell and the actual application requirements, and there is still huge room for future research in this area.

Whether it is O-SSOEC or H-SSOEC, the electrochemical performance of SSOEC is still worse than that of traditional anode-supported SOEC so far. A main reason is that the cell structure is supported by thick electrolyte (usually $>300\ \mu\text{m}$). Therefore, there is still a lot of work to do for improving cell performance about electrolyte.

Electrode

Symmetrical SOEC use the same electrode material as the anode and cathode, which put more stringent requirements on the material. The material must meet the requirements of the anode material and also meet the requirements of the cathode material:⁴⁷

- a. High electronic and ionic conductivity;
- b. High catalytic activity. The material must not only have good catalytic performance for H₂O or CO₂ reduction reaction (HER, CO₂RR), but also has good catalytic activity for oxygen evolution reaction (OER);
- c. High stability and compatibility. The material should have high stability (structural stability, phase stability, thermodynamic stability and chemical stability) both in oxidizing and reducing atmosphere. The material should have good stability towards H₂O and CO₂. It should also provide chemical and thermal compatibility with electrolyte and connectors. Besides, sufficient porosity for the transfer of fuel and specific surface area to provide enough active site for electro catalytic reaction are also important;
- d. Easy to manufacture and low cost.

In existing electrode materials, neither cathode materials nor anode materials can meet the requirements of symmetric electrode materials. Therefore, methods as changing the composition and microstructure of the electrode material, and adding new materials to prepare the composite electrode are adopted in order to meet the requirements of the symmetric electrode material. According to the structure of the

electrode material, it is divided into four categories, including simple perovskite (SP), double perovskite (DP), spinel oxide and other oxides as shown in the **Figure. 5** below.

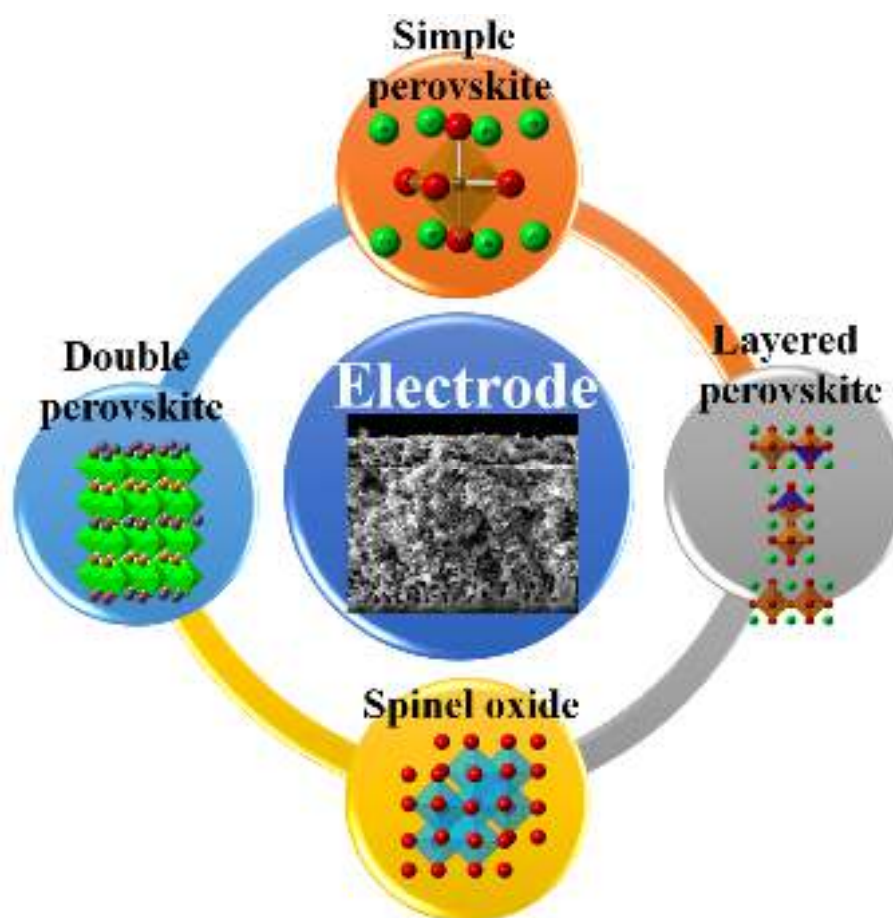


Figure 5. The main kinds of oxides of electrode for SSOEC.

Simple perovskite oxide (SP)

The simple perovskite oxide with the general formula ABO_3 is defined as an oxide with the same crystal structure as $CaTiO_3$. In general, rare earth ions with the large radius occupy the A-site that are 12-fold coordinated with oxygen ions, while the B-site is occupied by 6-fold coordinated transition metal ions. ⁷⁶ One characteristic of perovskite is that it can accommodate multiple A- and B-site cations. A variety of perovskite materials can be derived by doping or partial substitution at the A or B position. By adjusting the type and content of the A and B elements, the material

properties can be effectively adjusted, including redox stability, electrical conductivity, catalytic activity, etc., to meet specific application requirements.⁷⁷ In this case, perovskite materials have huge application prospects in photocatalysis, electrocatalysis, piezoelectric materials, thermoelectric materials and many other fields.^{12, 78-79}

Symmetrical electrode materials are first studied on the basis of connector materials. The LaCrO_3 based connector material with perovskite structure has good physical and chemical stability under different oxygen partial pressure and high electronic conductivity under oxidizing atmosphere. However, electronic conductivity of this connector material in a reducing atmosphere, as well as the catalytic activity of the material for hydrogen and oxygen, cannot satisfy the requirements.⁷⁷⁻⁷⁹ In order to make the connector material meet the requirements as a symmetric electrode material, from the direction of changing the electrode material structure, the researchers conducted the following research. $\text{La}_{0.75}\text{Sr}_{0.25}\text{Cr}_{0.5}\text{Mn}_{0.5}\text{O}_{3-\delta}$ (LSCM) were discovered by Tao et al. And used as SOFC anode materials to replace traditional Ni-YSZ anodes.⁸⁰ They revealed that the LSCM material is a mixed ionic and electronic conductivity (MIEC). The conductivity in air at 900 °C is $38.6 \text{ S}\cdot\text{cm}^{-1}$, and the conductivity in 5% H_2/N_2 is $1.49 \text{ S}\cdot\text{cm}^{-1}$.⁸¹ Most importantly, LSCM has good redox stability, resistance to sulfur poisoning and carbon deposition. In addition, LSCM materials are structurally stable under high temperature conditions and have excellent chemical compatibility with YSZ. Therefore, this redox-reversible oxide was used as an electrode for SSOECs.⁵⁹ LSCM electrode shows excellent performance with high current for activation both in air and CO_2 . Reduction of LSCM is the main process of low voltage during

electrolysis while reduction of CO₂ is the main process of high voltage. However, insufficient electrocatalytic activity of the LSCM still limits the cell performances and current efficiency. In order to improve the cell performances, the SSOECs based on LSCM loaded with 2 wt.% Fe₂O₃ was demonstrated.⁸² The loading of nano catalysts considerably enhances the electrode performance and the current efficiency of CO₂ electrolysis was accordingly enhanced by approximately 75% for the impregnated LSCM-based electrode at 800 °C. Scandium is doped into LSCM (La_{0.25}Sr_{0.75}Cr_{0.5}Mn_{0.4}Sc_{0.1}O_{3-δ}) to enhance the performance of the composite cathode.^[83] Faradic efficiency is accordingly enhanced by 20% and 50% compared with the electrolysis cell with LSCM cathode for high temperature steam electrolysis. In addition, LSCM based SSOECs is also used for steam/CO₂ co-electrolysis.⁸⁴ They can achieve the maximum density currents of 750 mA·cm⁻² and 620 mA·cm⁻² at 1.7 V for pure H₂O and for co H₂O-CO₂ electrolysis with ratios of 1:1, respectively. Generally, the electrical conductivity of the electrode should be at least 1 S·cm⁻¹ to reduce its ohmic loss. While LSCM is a p-type conductor, the concentration of charge carriers in LSCM will decrease because of the formation of oxygen vacancies at low pO₂. In addition, under high electrolytic voltage, LSCM has the potential of phase change or even to decomposition.⁸⁵

Fe-based perovskite materials have good ion-electron conductivity and excellent electrocatalytic performance. It has a lower coefficient of thermal expansion as compared to co-based perovskite materials and has better structural stability.⁸⁶⁻⁸⁸ Therefore, Fe-based perovskite materials are promising as electrodes of SSOEC.

$\text{La}_{0.6}\text{Sr}_{0.4}\text{Co}_{0.2}\text{Fe}_{0.8}\text{O}_3$ (LSCF), a commonly used SOEC anode material, also applied as an electrode for SSOEC. Their performance in high temperature H_2O electrolysis performance was investigated.⁸⁹ The over-potential of the LSCF-GDC cathode was found to have decreased significantly at a given current. Infiltration of GDC nanoparticles in LSCF electrode has improved the performance of SSOECs in CO_2 electroreduction,⁹⁰ whereas 10 wt.% GDC nanoparticle infiltration of the LSCF (10GDC/LSCF) electrode results in the highest performance. Mojie Cheng et al. reported a cell infiltrated with LSCF-GDC composite on YSZ scaffold as cathode and anode for CO_2 electrolysis,⁹¹ the cell obtains a current density of $1.01 \text{ A}\cdot\text{cm}^{-2}$ at 1.4 V and 800 °C, along with an CO production rate of $6.95 \text{ mL}\cdot\text{min}^{-1}\cdot\text{cm}^{-2}$ and Faraday efficiency of 98.8%. Moreover, they observed CO_2 electrolysis on LSCF-GDC cathode passes through two charge transfer reactions, in which the second charge transfer reaction from the intermediate carbonate reduction to CO is the key rate-determining step. Palladium (Pd) doped LSCF (LSCF-Pd) is a potential electrode of SSOEC. Current densities of more than 360 mA cm^{-2} were obtained at 800°C in electrolyte-supported tubular cells with high CO_2 and H_2O conversion to syngas.⁹² However, the stability of LSCF electrode materials in different working station has not been studied. In fact, LSCF can't maintain its structure in redox atmosphere. Therefore, the strategy of doping high-valence ions to stabilize LSCF has been studied. Co-electrolysis of H_2O - CO_2 in a SOEC with symmetrical $\text{La}_{0.4}\text{Sr}_{0.6}\text{Co}_{0.2}\text{Fe}_{0.7}\text{Nb}_{0.1}\text{O}_{3-\delta}$ (LSCFN) electrode has also been studied.⁹³ The current density can reach up to $0.638 \text{ A}\cdot\text{cm}^{-2}$ @1.3 V and 850 °C with the composition of 75% CO_2 -15% H_2O -10% H_2 and the cell demonstrates

excellent stability. Zhibin Yang et al investigated LSCFN perovskite oxide as electrode materials for SSOEC for CO₂ electrolysis with high current density and a low polarization resistance.⁹⁴ Owing to the reverse water gas shift reaction, cell performance of CO₂ electrolysis with H₂ as carrier gas is better than that with CO as carrier gas. However, the cobalt-containing oxides have a greater thermal expansion coefficient (TEC) than the YSZ electrolyte, which induces severe thermal stresses between the electrode and electrolyte, thereby weakening the charge exchange and mass transfer process.⁹⁵⁻⁹⁶ Besides that, the Co element can become volatile at high-temperature sintering, and Co is quite expensive. Hence, the development of cobalt-free electrodes is an essential requirement.

Co-free La_{0.3}Sr_{0.7}Fe_{0.7}Ti_{0.3}O₃ (LSFT) perovskite oxide is investigated as both anode and cathode materials in a SSOEC for direct electrolysis of pure CO₂ at 800 °C.⁹⁷ At an applied voltage of 2.0 V, the current density is 521 mA cm⁻². The symmetrical SOEC's lowest polarization resistance (R_p) is obtained at 2.0 V with a value as low as 0.08 cm². LSFT cathode also shows excellent durability in pure CO₂ electrolysis, particularly at high voltage of 2.0 V. The conventional electrode La_{0.8}Sr_{0.2}MnO_{3-δ} (LSM) was also used as an electrode of SSOEC for electrolysis CO₂ but resulted in unsatisfactory performance.⁹⁸

In our group, we are dedicated to the study of stable and excellent performance of ceramic oxide as electrodes for symmetrical cell. The SSOEC with a La_{0.6}Sr_{0.4}Fe_{0.8}Ni_{0.2}O_{3-δ} (LSFN)-GDC/GDC/YSZ/GDC/LSFN-GDC configuration was assessed for electrochemical performance in pure CO₂ electrolysis.⁹⁹ It is determined

that the current density is $1.03 \text{ A}\cdot\text{cm}^{-2}$ and the R_p is as low as $0.12 \Omega\cdot\text{cm}^2$ at $800 \text{ }^\circ\text{C}$ with the voltage of 2.0 V as shown in **Figure 6**. CO formation rates can reach $6.35 \text{ mL min}^{-1} \text{ cm}^{-2}$ at voltages of 2.0 V at $800 \text{ }^\circ\text{C}$, corresponding to high Faraday efficiency over 90% . Furthermore, the SSOEC also displayed high stability in the long-term CO_2 electrolysis test. The result confirms the proposed novel LSFN as a potential electrode material for pure CO_2 electrolysis in SSOECs. Although the LSFN symmetric cell has achieved good electrochemical performance, longer time operation should be carried out to confirm the reliability of LSFN materials in the future work.

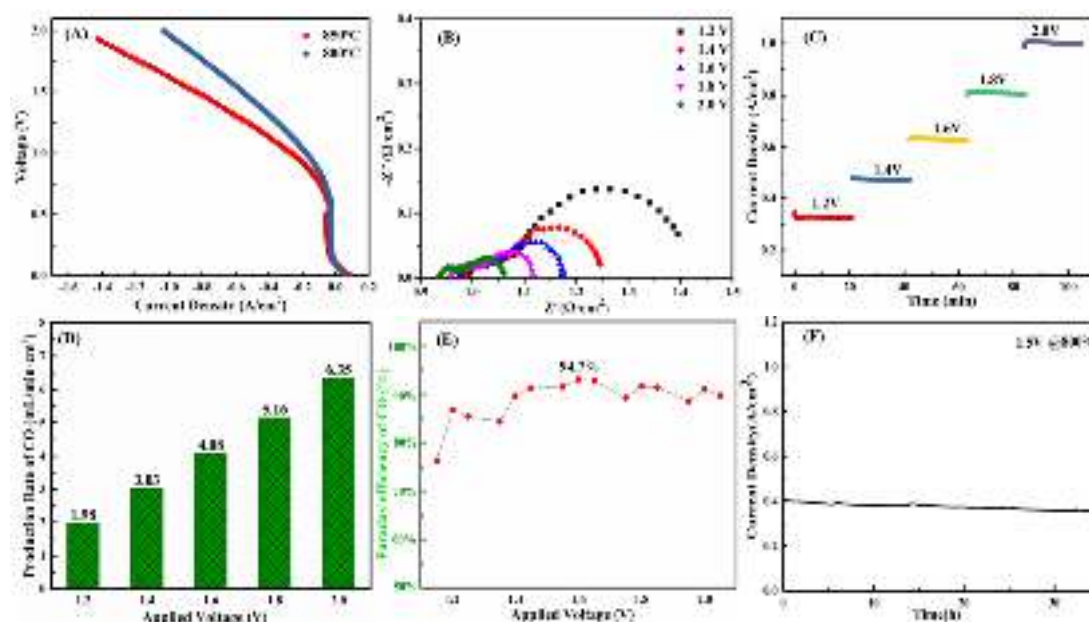


Figure 6. I-V curves of the LSFN symmetrical SOEC for pure CO_2 electrolysis at $800 \text{ }^\circ\text{C}$ and $850 \text{ }^\circ\text{C}$ (A); EIS of symmetrical SOEC under different voltages ($1.2\sim 2.0 \text{ V}$) for pure CO_2 electrolysis (B); Electrochemical performances of the symmetrical SOEC at $800 \text{ }^\circ\text{C}$. (C) potential static tests for CO_2 electrolysis at different applied voltages. (D) production rates of the CO ; (E) Faradic efficiency of CO_2 electrolysis at different applied voltages and (F) short-term durability test for pure CO_2 electrolysis at 1.5 V .⁹⁹

In order to enhance the performance LSFN electrode, we evaluated a novel quasi-symmetrical SOEC with reduced $\text{La}_{0.6}\text{Sr}_{0.4}\text{Fe}_{0.8}\text{Ni}_{0.2}\text{O}_{3-\delta}$ (R-LSFN) as cathode and LSFN as anode for pure CO_2 electrolysis¹⁰⁰. After reduction, Ni-Fe alloy nanoparticles are in-situ exsolved and oxygen vacancies are formed in LSFN lattices at the same time as shown in **Figure. 7 (A)**. The size of the nanoparticles is about 30 nm and it is tightly bound to the perovskite matrix. Compared to the LSFN symmetrical cell, the quasi-symmetrical cell with R-LSFN cathode shows current density of ($1.42\text{A}/\text{cm}^2$ vs $1.25\text{A}/\text{cm}^2$) at the applied voltage of 2.0 V under $850\text{ }^\circ\text{C}$ for CO_2 electrolysis, has lower polarization resistance ($0.06\ \Omega\cdot\text{cm}^2$ vs $0.09\ \Omega\cdot\text{cm}^2$), higher Faraday efficiency (98% vs 94%) and better long-term stability at $850\text{ }^\circ\text{C}$ as shown in **Figure. 7 (B)**. The enhancement mechanism is also discussed, which is due to the synergistic effect of the in-situ exsolved Ni-Fe nanoparticles and oxygen vacancies. The results suggest that the quasi-symmetrical SOEC with R-LSFN cathode demonstrate promising application for CO_2 electrolysis. It provides a new door to improve the performance of SSOEC by reducing the electrode on one side with this novel quasi-symmetrical structure.

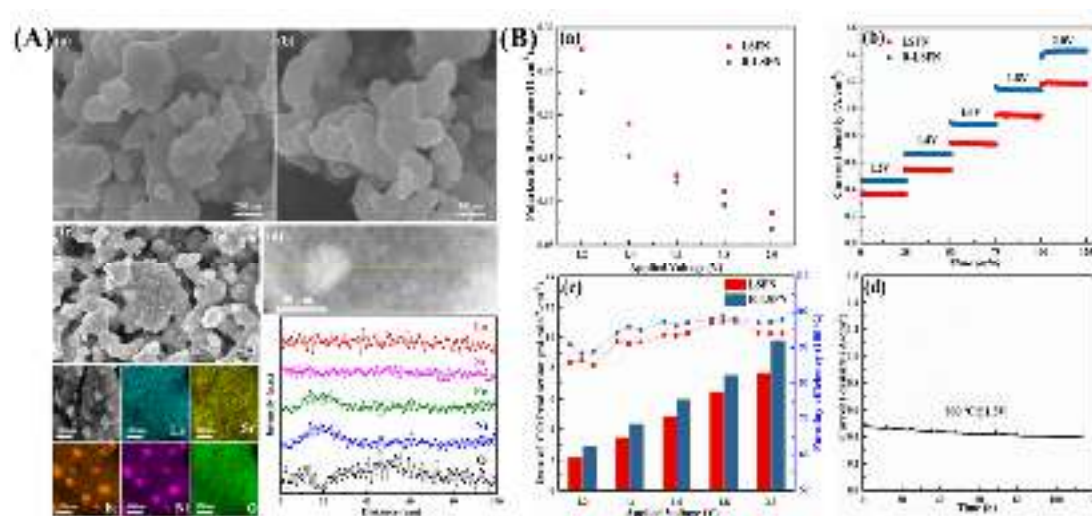


Figure 7. The morphology of LSFN and R-LSFN (A): the SEM images of LSFN (a)

and R-LSFN electrode (b), the EDS mapping of R-LSFN (c) and line scanning of R-LSFN (d); The electrochemical performance of R-LSFN quasi-symmetrical SOEC for CO₂ electrolysis: Polarization resistance of SSOEC under different voltage (a); short-term performance of CO₂ electrolysis at various voltage with LSFN cathode and R-LSFN cathode (b); the rate of CO production and Faraday efficiency at 850 °C (c) and long-term test of the R-LSFN cathode at 800 °C (d).¹⁰⁰ Copyright 2019, The ELSEVIER.

In addition, we also study the perovskite oxide La_{0.6}Sr_{0.4}Fe_{0.9}Mn_{0.1}O_{3-δ} (LSFM) as the electrode for direct high-temperature electrolysis of pure CO₂ in a SSOECs.¹⁰¹ The results confirm that LSFM as an excellent electrode material in a symmetrical SOEC for pure CO₂ electrolysis. However, segregation of the Sr element on the electrode surface, which radically deteriorate the electrode performance. When Sr-contained perovskite oxides are used as SOEC cathode for CO₂ electrolysis, they have a tendency to form the SrCO₃ layer on the electrode surface, causing the irreversible cell performance degradation.¹⁰²⁻¹⁰⁴ Similar performance degradation was noticed in our previous work, and one possible reason is that the Sr reacted with CO₂ to form SrCO₃ at the surface. In order to avoid the deleterious carbonate phase, Sr-free perovskite oxide La_{0.6}Ca_{0.4}Fe_{0.8}Ni_{0.2}O_{3-δ} (LCaFN) were developed and investigated as an electrode of SSOEC as shown in **Figure. 8**.¹⁰⁵ The polarization resistance of LCaFN in air and CO₂ are both lower than that of LSFN. For pure CO₂ electrolysis, LCaFN symmetrical cell achieves a maximum electrolysis current density of 1.41 A·cm⁻² at 800 °C under 2.0 V, and this value is larger than LCaFN asymmetrical cell (1.37 A·cm⁻²) and LSFN

symmetrical cell ($1.08 \text{ A} \cdot \text{cm}^{-2}$). Moreover, the polarization resistance of SSOEC is only $0.04 \text{ } \Omega \cdot \text{cm}^2$ and the cell has a high Faraday efficiency as shown in **Figure. 8 (A)**. Moreover, the LCaFN electrode shows good stability and can be recovered after a period of operation through simple air treatment whether it is a long-time interval or a short time interval, as shown in **Figure. 8 (B)**, indicating this material possesses the self-recovery ability. In fact, Ca in LCaFN lattice will inevitably diffuse to the surface under long-term high temperature operating conditions. On the one hand, CaO is a good idea to the adsorption of CO_2 . On the other hand, due to the lower decomposition temperature of CaCO_3 ($825 \text{ }^\circ\text{C}$), the electrode can be refreshed to the original state in the air because the CaCO_3 can be decomposed. Unfortunately, for LSFN cathode, once SrO reacts with CO_2 to form SrCO_3 , it is very difficult to decompose the stable SrCO_3 due to their higher decomposition temperature ($1200 \text{ }^\circ\text{C}$). Therefore, SrCO_3 will continue to grow and deposits on the surface and reduces electrochemical active sites, leading to irreversible performance degradation. This work proves that doping Ca at A site is beneficial for CO_2 electrolysis.

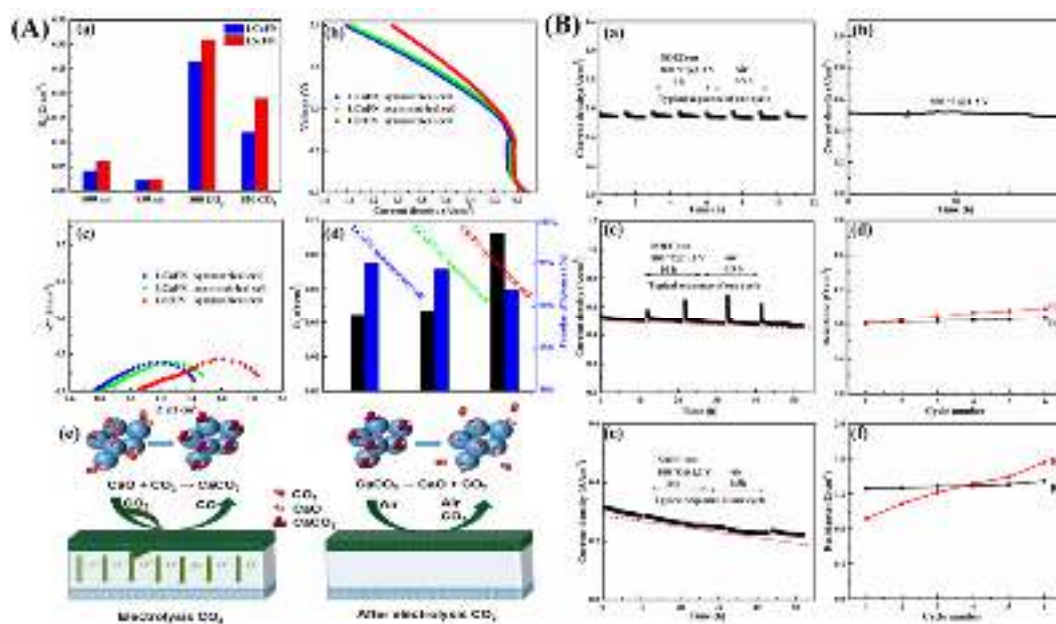


Figure 8. The electrochemical performance of three cells (A): R_p of LCaFN and LSFN electrode under air and CO₂ atmosphere (a), I-V curves of LCaFN symmetrical cell, LCaFN asymmetrical cell and LSFN symmetrical cell for pure CO₂ electrolysis (b), EIS of three cells (c), R_p and Faraday efficiency of three cells at applied voltage of 2.0 V at 800 °C (d), the schematic diagrams of the self-recovery of LCaFN electrode in CO₂ electrolysis at 800 °C; The self-recovery performance of LCaFN cells (B): The cyclic test (short time interval 1 h) (a), 40 h durability test (b), the cyclic test (long time interval 10 h) and resistance of the LCaFN symmetrical cell (c, d), the cyclic test (long time interval 10 h) and resistance of LSFN symmetrical cell (e, f).¹⁰⁵ Copyright 2019, The Royal Society of Chemistry.

Double perovskite oxide (DP)

Double perovskite oxides (DP) with a formula of AA'B₂O₆ (where A are rare-earth metals, A' are alkali or alkaline earth metals and B are a transition metals) possess superior mixed ionic conductivities and high oxygen surface exchange coefficient due to their special crystal structure, showing a [AO]-[BO]-[A'O]-[BO]-stacking

sequence. The oxygen vacancies are primarily located in the [AO] planes. Excellent cell performance has been achieved by using these materials.¹⁰⁶⁻¹⁰⁸ This type of material has high ionic conductivity, oxygen diffusion coefficient, and oxygen surface conversion coefficient compared to traditional perovskite cathode materials; it is also possible to dope different elements to tune the electronic conductivity and TEC. A novel type of perovskite electrode material $\text{SrFe}_{1-x}\text{Mo}_x\text{O}_3$ has widely grabbed the attention as it has high electronic conductivity and good redox stability in both air and fuel atmospheres, which aptly fits the requirements of a symmetric electrode material. For the first time in SSOECs, perovskite oxide $\text{Sr}_2\text{Fe}_{1.5}\text{Mo}_{0.5}\text{O}_{6-\delta}$ (SFM) was considered to be both anode and cathode for hydrogen production.¹⁹ At 900 °C, with an electrolysis voltage of 1.3 V and 60 vol % AH, an electrolysis current of 0.88 A cm^{-2} and a hydrogen production rate up to 380 mL $\text{cm}^{-2} \text{h}^{-1}$ can be achieved. The cell also demonstrated good stability in the long-term H_2O electrolysis test. SFM performance has proven to be a promising alternative electrode of SSOEC for $\text{H}_2\text{O}/\text{CO}_2$ co-electrolysis process.¹⁰⁹ The cell shows a current density of 0.734 A $\cdot \text{cm}^{-2}$ at 850 °C. Syngas with CO_2 conversion rate of 0.58 and H_2 to CO ratio of 2 has been achieved by adjusting the inlet gas fraction. A novel SSOEC was prepared by a facile tape-casting and infiltration method.¹¹⁰ It can achieve a current density of 1.24 A $\cdot \text{cm}^{-2}$, which could be related to the significantly extended active sites resulting from novel architecture with infiltrated SFM nano-networks. This strategy seems to be a promising approach to produce unique architecture with SSOECs. Furthermore, in situ grown Fe-ceramic composite cathode after reduced can augment triple-phase boundaries (TPB) for the $\text{H}_2\text{O}/\text{CO}_2$ co-

electrolysis process.¹¹¹ Thus 10% Fe has been doped in the B-site of $\text{Sr}_2\text{Fe}_{1.6}\text{Mo}_{0.5}\text{O}_{6-\delta}$. At 1.6 V and 850 °C, the current density achieves $1.27 \text{ A}\cdot\text{cm}^{-2}$ using the $\text{Sr}_2\text{Fe}_{1.6}\text{Mo}_{0.5}\text{O}_{6-\delta}$ -SDC/LSGM/SFM-SDC configuration of solid oxide cells. The highest current efficiency of ~91% is attained at 1.3 V. The cell shows highly stable performance even after 100 h operations. SFM electrodes are deposited on both sides of the GDC coated YbScSZ tapes.¹¹² In addition to SFM, another double perovskite $(\text{PrBa})_{0.95}(\text{Fe}_{0.9}\text{Mo}_{0.1})_2\text{O}_{5+\delta}$ (PBFM) as electrode materials was studied for high-performance SSOECs.¹¹³ At 800 °C, the PBFM/LSGM/PBFM-configured SOEC exhibits a relatively high current density of 510 mA cm^{-2} at 1.3 V.

Apart from the A-site ordering double perovskite, B-site ordering double perovskite like $\text{Sr}_2\text{Ti}_{0.8}\text{Co}_{0.2}\text{FeO}_6$ (STC02F) was also fabricated as symmetrical electrode for SOFC and SOEC.¹¹⁴ STC02F is capable of exsolving Co-Fe alloy nanoparticles in reducing conditions and ensures perovskites structural stability. STC02F based symmetric solid oxide cell exhibited exceptional performance in various fuel and co-electrolysis $\text{H}_2\text{O}/\text{CO}_2$. Moreover, STC02F symmetrical electrode operating in SOFC and SOEC model shows satisfying electrochemical stability.

However, only the aforementioned double perovskite oxides are used for the electrodes of SSOECs so far, compared with the simple perovskite oxides electrode, the research on double perovskite oxides electrode is still relatively minor. However, the double perovskite oxides such as $\text{PrBa}_{0.8}\text{Ca}_{0.2}\text{Co}_2\text{O}_{5+\delta}$ (PBCC), $\text{PrBa}_{0.5}\text{Sr}_{0.5}\text{Co}_{1.5}\text{Fe}_{0.5}\text{O}_{5+\delta}$ (PBSCF), $\text{SmBa}_{0.5}\text{Sr}_{0.5}\text{Co}_2\text{O}_{5+\delta}$ (SBSC) have been widely used in the cathode and anode of SOCs.¹¹⁵⁻¹¹⁷ In the future research, we can learn from

the research strategy of single perovskite oxide, through doping, coating modification, exsolution or other technical means to further improve the electrocatalytic performance and stability of double perovskite materials.

Spinel oxide

Spinel oxides with the composition AB_2O_4 (where A and B are metal ions) have formed a very large family and may contain one or more metal elements. Almost all of the main group and transition metal can exist in the spinel phase. Spinel oxides have shown intrinsic magnetic,¹¹⁸ optical,¹¹⁹ electrical¹²⁰ and catalytic properties¹²¹ owing to their variable compositions, electron configurations and valence states. A spinel oxide $MnCo_2O_4$ electrode-based SSOEC is studied for pure CO_2 electrolysis.¹²² The electrode is prepared by the impregnation method; the cell attained a current density of 0.75 A cm^{-2} with 1.5 V at $800\text{ }^\circ\text{C}$. Also, the $MnCo_2O_4$ electrodes exhibited excellent stability when operated for more than 80 h during pure CO_2 electrolysis. Another electrode with $Ni(Mn_{1/3}Cr_{2/3})_2O_4$ (NMC) spinel oxides composite GDC are also adopted for SSOCs and their applicability are demonstrated successfully in both SOFC and SOEC modes.¹²³ NMC can be decomposed to Ni and other spinel oxide under H_2 or CO, but it would quickly recuperate to NMC in air or pure CO_2 atmosphere. Moreover, NMC–GDC composite electrodes display a high redox resistance and rapid recovery. This is mainly due to the significant difference in Gibbs free energy of NMC in reducing and oxidizing atmospheres as shown in **Figure. 9 (A)**. Faradaic efficiency of over 96% at $700\text{--}850\text{ }^\circ\text{C}$ and the electrolysis current density of $2320\text{ mA}\cdot\text{cm}^{-2}$ at $850\text{ }^\circ\text{C}$ can be achieved in SOEC mode as shown in **Figure. 9 (B)**. Furthermore, it is

worth noting that the voltage decreased from 1.507 V to 1.407 V during the stability test as shown in **Figure. 9 (D)**. The reason may be the nickel exsolved in a reduction atmosphere. In addition, the NMCs has the multi-functionality due to the abundant transition metal element centered octahedra. The results indicated that NMC shows outstanding redox resistance and running stable. This work is anticipated to play a pivotal role in the future exploration of novel and stable spinel oxide electrodes for solid oxide cells. Because we usually think that spinel oxide is unstable under high temperature conditions. In fact, developing electrode materials with both well electrochemical performance and good stability is the research hotspots, but the most effective way is to get a delicate balance between them.

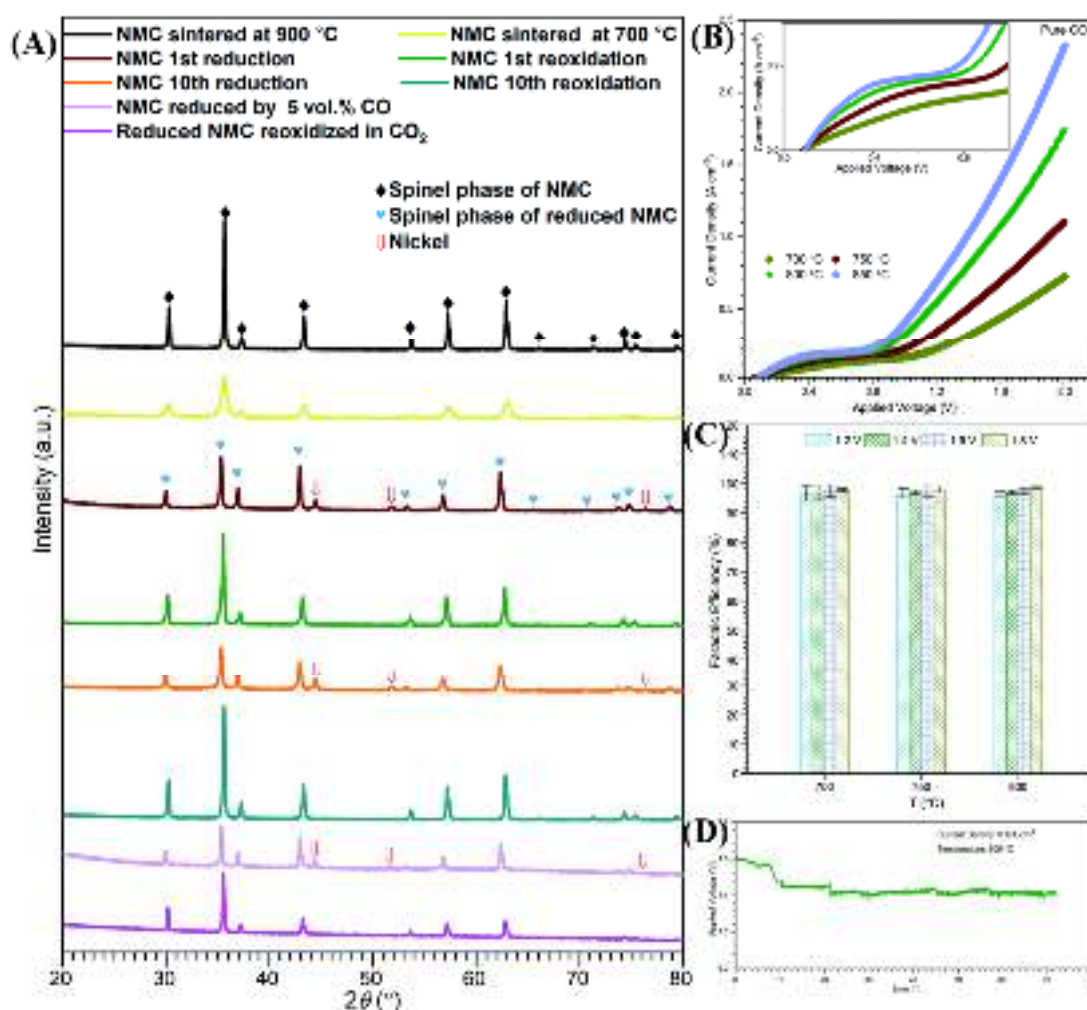


Figure 9. The XRD results of NMC synthesized at different temperatures and processed in different atmospheres (A), I-V curves of the symmetrical cell (NMC–GDC/YSZ/NMC–GDC) fueled with pure CO₂ in the cathode at 650–850 °C (B), The faradaic efficiencies of the symmetrical cell at different applied voltages and temperatures (C), The V–t curves of the symmetrical cell at an electrolysis current density of 0.8 A·cm⁻² at 800 °C (D).¹²³ Copyright 2020, The Royal Society of Chemistry.

Not only in the field of symmetrical electrolysis cells, even in the field of solid oxide cells, there are relatively few studies on spinel oxides so far. The main reason is that most of the spinel oxides are structurally unstable at high temperature and in a reducing atmosphere. In the future research, we think the electrocatalytic activity and stability of spinel oxides can be furthermore improved by constructing a core-shell structure through drawing on existing electrode research. In our group, La₂NiO_{4-δ} coated PBSCF composite cathode with core-shell structure was prepared and used as the cathode of SOFC, which can improve the stability and electrocatalytic activity of the electrode.¹²⁴ In addition, La_{0.8}Sr_{0.2}MnO_{3-δ} coated Ba_{0.5}Sr_{0.5}Co_{0.8}Fe_{0.2}O_{3-δ} was also investigated with the same core-shell structure.¹²⁵ Therefore, core-shell structure can improve the stability of electrodes.

Reversible symmetrical solid oxide electrolysis cells

Reversible solid oxide electrolysis cells (RSOECs) have been favored for their high efficiency and ecological compatibility.¹²⁶⁻¹²⁸ They can convert the fuels (H₂, CO, CH₄ et al) chemical energy into clean electric energy in the fuel cell mode, or use the

non-continuous clean energy (wind, solar, tidal energy, etc.) to electrolyze H₂O or CO₂ in the electrolysis mode for energy storage. In general, SSOEC can both work in SOFC mode for power output, and it also can work in SOEC mode for energy storage. Reversible symmetrical solid oxide electrolysis cell (RSSOECs) has drawn significant attention for energy conversion and storage. GDC-infiltrated La_{0.3}Ca_{0.7}Fe_{0.7}Cr_{0.3}O_{3-δ} (LCFC) symmetrical electrodes were first studied for reversible SSOECs.¹²⁹ It has achieved admirable activity towards the oxygen reduction and oxygen evolution reactions. Similar electrode La_{0.3}Sr_{0.7}Fe_{0.7}Cr_{0.3}O_{3-δ} (LSFCr-3) was studied using the 3-electrode half-cell configuration in a different atmosphere. The results indicated that the oxygen reduction being slightly worse than that of oxygen evolution, and CO₂ reduction more active than CO oxidation.¹³⁰ LSFCr/GDC/YSZ/GDC/LSFCr cells make a highly effective and stable towards CO₂ electrolysis (SOEC mode) and the oxidation of CO (SOFC mode). Moreover, cell performance during the electrolysis of CO₂ is higher than for the oxidation of CO.¹³¹

In order to improve material processing and cell manufacturing methods in RSSOECs. Viola Birss et al. first reported the fabrication of a SSOEC based on LCFC using rapid, low-cost, low-energy, and green microwave processing techniques.^[132] In addition, highly active ceramic symmetrical electrode La_{0.3}Sr_{0.7}Ti_{0.3}Fe_{0.7}O_{3-δ}-CeO₂ for RSSOECs has been studied. A well-deposited microstructure is observed in the infiltrated electrode. Maximum current density of 1.90 A·cm⁻² at 2.0 V can be obtained from the I–V curves, at CO: CO₂ ratio of 1: 1 for CO₂ electrolysis at 850 °C, whereas the corresponding power density is 357 mW·cm⁻² in SOFC mode under the similar

operating conditions.⁶⁰ Co-free $\text{La}_{0.5}\text{Sr}_{0.5}\text{Fe}_{0.9}\text{Nb}_{0.1}\text{O}_{3-\delta}$ (LSFNb) was synthesized and used as an electrode of RSSOC.¹³³ The maximum power density can be achieved $1.157 \text{ W}\cdot\text{cm}^{-2}$ at $850 \text{ }^\circ\text{C}$ in SOFC mode, while the electrolysis current density is $1.46 \text{ A}\cdot\text{cm}^{-2}$ at 1.3 V in SOEC mode. In addition, the H_2 and CO production rates are 2.19 and $2.77 \text{ mL}\cdot\text{min}^{-1}\cdot\text{cm}^{-2}$ with nearly 100% Faradaic efficiency for $\text{H}_2\text{O}/\text{CO}_2$ Co-electrolysis at $800 \text{ }^\circ\text{C}$. Moreover, the symmetric cell displays good stability under $\text{CO}_2\text{-H}_2\text{O}$ co-electrolysis. Both these results indicate that LSFNb symmetrical cell has promising application prospect for $\text{H}_2\text{O}/\text{CO}_2$ co-electrolysis as well as for regenerative fuel cells.

To achieve a high-performance cell, Guntae Kim et al. designed a ‘self-transforming cell’ with the asymmetric configuration using only single type materials, one based on atmospheric adaptive materials.¹³⁴ Atmospheric adaptive perovskite oxide $\text{Pr}_{0.5}\text{Ba}_{0.5}\text{Mn}_{0.85}\text{Co}_{0.15}\text{O}_{3-\delta}$ (PBMCo) was used as self-transforming cell electrodes, which in the fuel atmosphere changed into layered perovskite and metal, and retained its original structure in the air atmosphere as shown in **Figure. 10**. In SOFC mode, the self-transforming cell displays excellent electrochemical performance of $1.10 \text{ W}\cdot\text{cm}^{-2}$ at $800 \text{ }^\circ\text{C}$ and good stability for 100 h without any catalysts. In SOEC mode, moderate current densities of $0.42 \text{ A}\cdot\text{cm}^{-2}$ for 3 vol.% H_2O and $0.62 \text{ A}\cdot\text{cm}^{-2}$ for 10 vol.% H_2O , respectively, were observed at a cell voltage of 1.3V at $800 \text{ }^\circ\text{C}$. The transforming cell maintains the constant voltages for 30 h in the reversible cycling test at $\pm 0.2 \text{ A}\cdot\text{cm}^{-2}$ and 10 vol. % H_2O . The “self-transforming cell” is similar to the concept of quasi-symmetrical cell we mentioned earlier. It can be concluded that the quasi-symmetric cell can effectively improve the electrochemical performance of the cell.

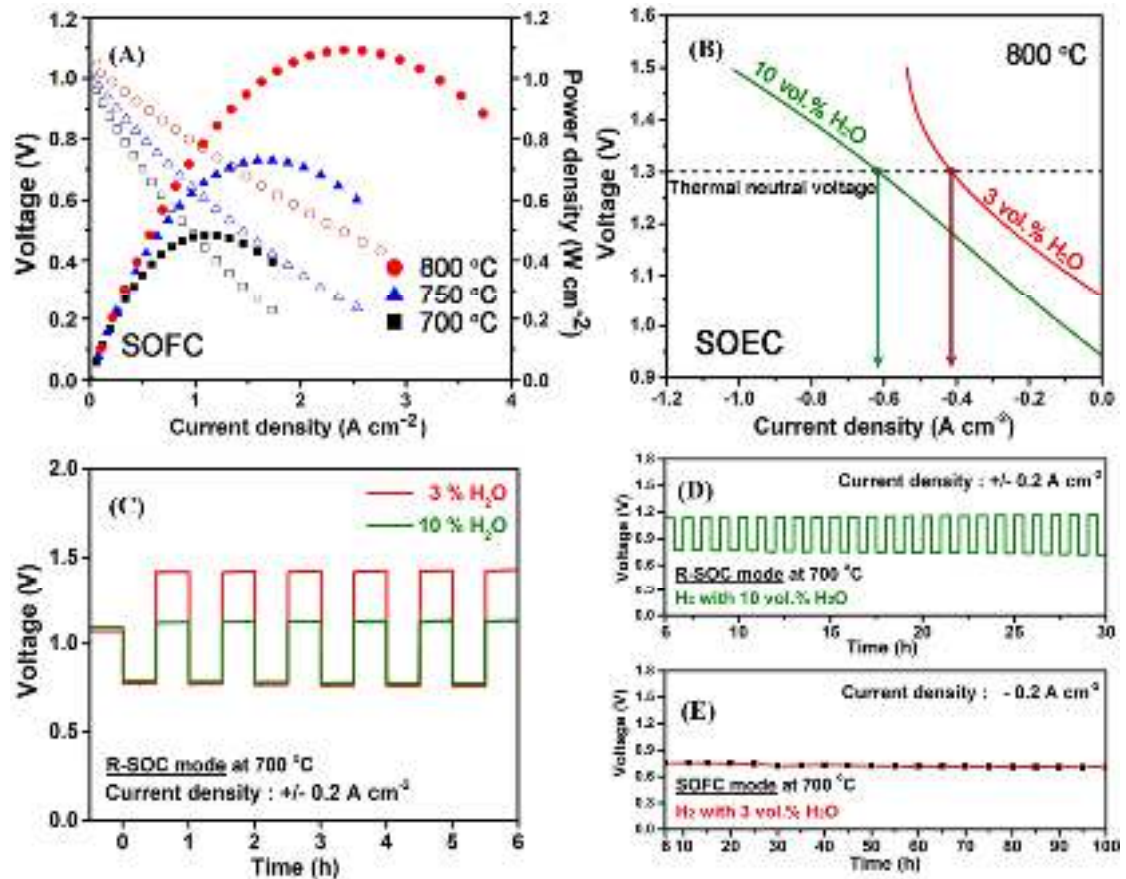


Figure 10. (A) Voltage-current density and corresponding power density curves of the transforming cell at 800, 750, 700 °C using humidified H₂ (3% H₂O). (B) Voltage-current density curves of the transforming cell at 800 °C under electrolysis mode with 3% and 10% H₂O containing H₂ safe gas. (C) Long-term stability of the transforming cell at 700 °C with current density of $-0.2 A \cdot cm^{-2}$. (D) The reversible cycling result performed at $-0.2 A \cdot cm^{-2}$ (electrolysis mode) and at $0.2 A \cdot cm^{-2}$ (fuel cell mode) and the long term test of SOFC (E).¹³⁴ Copyright 2018, The Nature.

A nominated Sr₂Fe_{1.5}Mo_{0.5}O_{6-δ} (SFM) is deposited onto porous YSZ backbone via an infiltration process.¹³⁵ In SOFC mode, the two corresponding cells exhibit good performance with maximum power densities of 0.218 and 0.265 $W \cdot cm^{-2}$, respectively. In SOEC mode, the current densities are 0.573 and 0.618 $A \cdot cm^{-2}$ when 1.5 V is

implemented. Applying SFM-GDC symmetrical electrode, the 300 μm -thick YSZ electrolyte-supported RSOECs with GDC buffer layers show acceptance electrochemical performance and can seamlessly switch between power generation and electrolysis modes with no obvious degradation after 20 h of short-term stability test working under humidified (3% H_2O) H_2 and 3% H_2O -air atmospheres, respectively. ^[136] Cu-based cermet suitable for electrodes in RSSOECs based on the GDC electrolyte were developed. ¹³⁷ The high stability, reversibility, catalytic activity and electrochemical performance make these electrodes promising for RSSOECs. A-site deficient $(\text{La}_{0.8}\text{Sr}_{0.2})_{0.9}\text{Sc}_{0.2}\text{Mn}_{0.8-x}\text{Ru}_x\text{O}_{3-\delta}$ can serve simultaneously as an air electrode and a fuel electrode in RSSOECs. ¹³⁸ Ru nanoparticle catalysts are exsolved on the surface of $(\text{La}_{0.8}\text{Sr}_{0.2})_{0.9}\text{Sc}_{0.2}\text{Mn}_{0.8-x}\text{Ru}_x\text{O}_{3-\delta}$ in the reducing atmospheres. Ru-doping significantly enhances the electrochemical activity of both the air electrode and the fuel electrode. In SOFC mode, the maximum power density of the symmetrical single cell reaches $0.318 \text{ W}\cdot\text{cm}^{-2}$ at $800 \text{ }^\circ\text{C}$. In SOEC mode, the electrolysis current density is $0.536 \text{ A}\cdot\text{cm}^{-2}$ at $750 \text{ }^\circ\text{C}$ at an applied voltage of 1.5 V at 50% $\text{H}_2\text{O}/\text{H}_2$.

We have summarized the electrode that have been used in SSOEC for H_2O electrolysis, CO_2 electrolysis or Co-electrolysis as shown in **Table 2**. We found the Fe based perovskite oxides and double perovskite oxides displayed exciting electrolysis current density. Moreover, infiltration and in-situ exsolution method also can improve the electrochemical performance of the electrode.

Table 2 The summarized performance of SSOEC with different electrodes.

Electrode	Electrolyte	Thickness (μm)	Test conditions	Current density (A/cm^2)	R_p ($\Omega \cdot \text{cm}^2$)	R_p @ Air	Ref
$\text{La}_{0.75}\text{Sr}_{0.25}\text{Cr}_{0.5}\text{Mn}_{0.5}\text{O}_{3-\delta}$ -SDC	YSZ	2000	800@CO ₂	0.018@2.0V	2@2.0V	0.325	59
$\text{La}_{0.3}\text{Sr}_{0.7}\text{Ti}_{0.3}\text{Fe}_{0.7}\text{O}_{3-\delta}$ -CeO ₂	SSZ	70	850@CO/CO ₂ 50:50	1.90@2.0V	0.28@OCV		60
LSCrM-SDC-Fe ₂ O ₃	YSZ	2000	800@CO ₂	0.38@2.0V	0.6@2.0V	0.35	82
$\text{La}_{0.25}\text{Sr}_{0.75}\text{Cr}_{0.5}\text{Mn}_{0.4}\text{Sc}_{0.1}\text{O}_{3-\delta}$	YSZ	2000	700@ 5H ₂ O	0.075@2.0V	6.5@1.8V	2.4	83
$\text{La}_{0.75}\text{Sr}_{0.25}\text{Cr}_{0.5}\text{Mn}_{0.5}\text{O}_{3-\delta}$	YbScSZ	165	850@H ₂ O/CO ₂	0.62@1.7V			84
$\text{La}_{0.6}\text{Sr}_{0.4}\text{Co}_{0.2}\text{Fe}_{0.8}\text{O}_{3-\delta}$ -GDC	SSZ	200	800@H ₂ O/CO ₂	0.36@1.6V			89
$\text{La}_{0.6}\text{Sr}_{0.4}\text{Co}_{0.2}\text{Fe}_{0.8}\text{O}_{3-\delta}$ -GDC (impregnation)	YSZ	300	800@CO ₂	0.555@1.6V	0.225@1.6V		90
$\text{La}_{0.6}\text{Sr}_{0.4}\text{Co}_{0.2}\text{Fe}_{0.8}\text{O}_{3-\delta}$ -GDC (impregnation)	YSZ	150	800@CO ₂ /CO	1.01@1.4V	0.45@1.4V		91
Pd- $\text{La}_{0.6}\text{Sr}_{0.4}\text{Co}_{0.2}\text{Fe}_{0.8}\text{O}_{3-\delta}$	YSZ	800	800@CO ₂	0.3@1.6V	1.12@1.6V	0.07@1.6V	92
$\text{La}_{0.4}\text{Sr}_{0.6}\text{Co}_{0.2}\text{Fe}_{0.7}\text{Nb}_{0.1}\text{O}_{3-\delta}$	YSZ	500	850@75CO ₂ /15H ₂ O	0.638@1.3V	0.42@OCV		93
$\text{La}_{0.4}\text{Sr}_{0.6}\text{Co}_{0.2}\text{Fe}_{0.7}\text{Nb}_{0.1}\text{O}_{3-\delta}$	YSZ	200	800@CO ₂	0.442@1.5V	0.68@OCV		94
$\text{La}_{0.3}\text{Sr}_{0.7}\text{Fe}_{0.7}\text{Ti}_{0.3}\text{O}_3$	YSZ	700	800@CO ₂	0.521@2.0V	0.08@2.0V		95
$\text{La}_{0.8}\text{Sr}_{0.2}\text{MnO}_{3-\delta}$	YSZ	700	750@CO ₂ /H ₂ =92/8	0.28@2.5V	17.2@OCV		98
$\text{La}_{0.6}\text{Sr}_{0.4}\text{Fe}_{0.8}\text{Ni}_{0.2}\text{O}_{3-\delta}$ -GDC	YSZ	400	850@CO ₂	1.52@2.0V	0.12@2.0V	0.025	99
Fe-Ni- $\text{La}_{0.6}\text{Sr}_{0.4}\text{Fe}_{0.8}\text{Ni}_{0.2}\text{O}_{3-\delta}$	YSZ	300	850@CO ₂	1.42@2.0V	0.06@2.0V		100
$\text{La}_{0.6}\text{Sr}_{0.4}\text{Fe}_{0.9}\text{Mn}_{0.1}\text{O}_{3-\delta}$	YSZ	200	800@CO ₂	1.107@2.0V	0.068@2.0V	0.24	101
$\text{La}_{0.6}\text{Ca}_{0.4}\text{Fe}_{0.8}\text{Ni}_{0.2}\text{O}_{3-\delta}$	YSZ	300	800@CO ₂	1.41@2.0V	0.04@2.0V	0.03	105
$\text{Sr}_2\text{Fe}_{1.5}\text{Mo}_{0.5}\text{O}_{6-\delta}$ -SDC	LSGM	502	850@H ₂ O/CO ₂	0.734@1.3V	0.48@OCV		109
$\text{Sr}_2\text{FeMoO}_6$ (impregnation)	LSGM	15	800@CO ₂	1.24@1.5V	0.226@OCV	0.064	110
$\text{Sr}_2\text{Fe}_{1.6}\text{Mo}_{0.5}\text{O}_{6-\delta}$ -SDC	LSGM	300	850@H ₂ O/CO ₂ =1/1	1.27@1.6V	0.29@1.3V		111
$\text{Sr}_2\text{Fe}_{1.5}\text{Mo}_{0.5}\text{O}_{6-\delta}$	6Yb4ScSZ	280	900@90H ₂ O/10Ar	1.4@1.3V	0.13@OCV	0.15	112
(PrBa) _{0.95} (Fe _{0.9} Mo _{0.1}) ₂ O _{5+δ}	LSGM	450	800@3H ₂ O/97H ₂	0.51@1.3V	1.5@OCV		113
$\text{Sr}_2\text{Ti}_{1-x}\text{Co}_x\text{FeO}_6$	LSGM	270	800@50H ₂ O/50H ₂	0.46@1.3V	0.124		114
Ni(Mn _{1/3} Cr _{2/3}) ₂ O ₄ -GDC	YSZ	250	800@CO ₂	1.74@0.2V	0.17@2.0V		123
$\text{La}_{0.3}\text{Sr}_{0.7}\text{Fe}_{0.7}\text{Cr}_{0.3}\text{O}_{3-\delta}$	YSZ	300	800@CO ₂ /CO90:10	0.41@1.5V	0.87@OCV		131
$\text{La}_{0.5}\text{Sr}_{0.5}\text{Fe}_{0.9}\text{Nb}_{0.1}\text{O}_{3-\delta}$	LSGM	250	850@H ₂ O/CO ₂ 2:8	1.46@1.3V	0.09@1.3 V	0.26	133
$\text{Pr}_{0.5}\text{Ba}_{0.5}\text{Mn}_{0.85}\text{Co}_{0.15}\text{O}_{3-\delta}$	LSGM	300	800@10%H ₂ O	0.62@1.3V	0.14@OCV	0.033	134
$\text{Sr}_2\text{Fe}_{1.5}\text{Mo}_{0.5}\text{O}_6$ (impregnation)	YSZ	100	750@CO:CO ₂ 50:50	0.618@1.5V	0.434@1.5V	0.064	135
$\text{Sr}_2\text{Fe}_{1.5}\text{Mo}_{0.5}\text{O}_{6-\delta}$ -GDC	YSZ	300	750@3%H ₂ O	0.202@1.3V	0.53@OCV		136
(La _{0.8} Sr _{0.2}) _{0.9} Sc _{0.2} Mn _{0.8-x} Ru _x O _{3-δ}	SSZ	200	750@50H ₂ O/50H ₂	0.536@1.5V		0.23	138

Recent developments in H-SSOEC

H-SOECs have gradually gained research attention in recent years, chiefly because

of the unique merits of H-SOECs over O-SOECs, such as lower operation temperature (500–700 °C), lower activation energy of proton, and ease of gas separation.^{55, 139-140} Compared to O-SSOECs, H-SSOECs are significantly less prevalent in the literature and the development of H-SSOECs is still the preliminary phase.

Kui Xie et al. reported a novel H-SSOEC with redox-stable LSCM electrode for the electrochemical conversion of CO₂/H₂O into syngas (CO/H₂).⁷² LSCM is impregnated with Ru catalyst to improve the electrode activity. Electrochemical measurements demonstrate that the CO₂ is electrochemically reduced to syngas (CO/H₂) with simultaneous H₂O electrolysis. The loading of Ru catalyst promotes the electrochemical process with higher Faradic efficiency while induces a more competitive process of hydrogen evolution at 700 °C. electrolysis of H₂O/CO₂ in SSOEC with barium cerate-carbonate composite electrolyte was also studied.¹⁴¹ The application of composite electrolytes promotes the transport of protons and directly leads to the production of H₂, even CH₄. To some extent, carbon resistance ensures the SSOEC operation at a lower bias potential of 0.5 V (vs OCV) applied. A redox-stable and carbon-tolerant LSCM as symmetric electrode with a hybrid-ion-conducting composite electrolyte achieves the fuel synthesis by CO₂ reduction in H-SOEC. The cell fabricated on the basis of P–N–BCZD|BCZD|PBN–BCZD (where BCZD = BaCe_{0.5}Zr_{0.3}Dy_{0.2}O_{3-δ}, PBN = Pr_{1.9}Ba_{0.1}NiO_{4+δ}, P = Pr₂O₃, N = Ni) is investigated at different temperatures and water vapor partial pressures (pH₂O).¹⁴² The SOEC mode of this cell is considered to be more appropriate than the SOFC mode in high humidified atmospheres, since its improved performance is determined by the ohmic resistance,

which decreases with an increase in $p_{\text{H}_2\text{O}}$. Jun Zhou et al reported a highly active Ruddlesden-Popper oxide as a symmetrical electrode for RSOEC via in-situ exsolution strategy.¹⁴³ A simple reduction procedure can produce the Cu nanoparticle-decorated $(\text{LaSr})_{0.9}\text{Fe}_{0.9}\text{Cu}_{0.1}\text{O}_4$ (LSFCu) oxide. The LSFCu shows a highly electrocatalytic activity toward ORR and HOR respectively as shown in **Figure. 11 (A, B)**. In SOFC mode, the peak power densities are $0.573 \text{ W}\cdot\text{cm}^{-2}$ and $0.396 \text{ W}\cdot\text{cm}^{-2}$ at $800 \text{ }^\circ\text{C}$ using humidified H_2 and CH_4 as fuel, respectively as shown in **Figure. 11 (C)**. Moreover, an exceedingly high current density of $1.02 \text{ A}\cdot\text{cm}^{-2}$ can be accomplished at 1.2 V in SOEC mode as shown in **Figure.11 (D)**. This work demonstrates a novel strategy to converse various energies using H-SSOCs. $\text{BaCo}_{0.4}\text{Fe}_{0.4}\text{Zr}_{0.1}\text{Y}_{0.1}\text{O}_3$ (BCFZY) perovskite oxide has been considered to be an outstanding electrode for H-SOC with achieving excellent electrochemical performance.¹⁴⁴⁻¹⁴⁵ This material was also employed as an electrode of symmetrical H-SOFC for low temperature and high-performance application.¹⁴⁶ Quasi-SSOFCs with $480 \mu\text{m}$ thick BZCY electrolyte and $25 \mu\text{m}$ thick electrode deliver a peak power density of 0.1148 and 0.0743 W cm^{-2} at 650 and $600 \text{ }^\circ\text{C}$, respectively. Additionally, SSOFC also displays acceptable durability under constant voltage operational condition for 25 h . However, there is no reported research into its electrochemical performance in SOEC mode. Considering its superior electrolytic catalytic activity, it is worth investigating the electrochemical performance in SOEC mode.

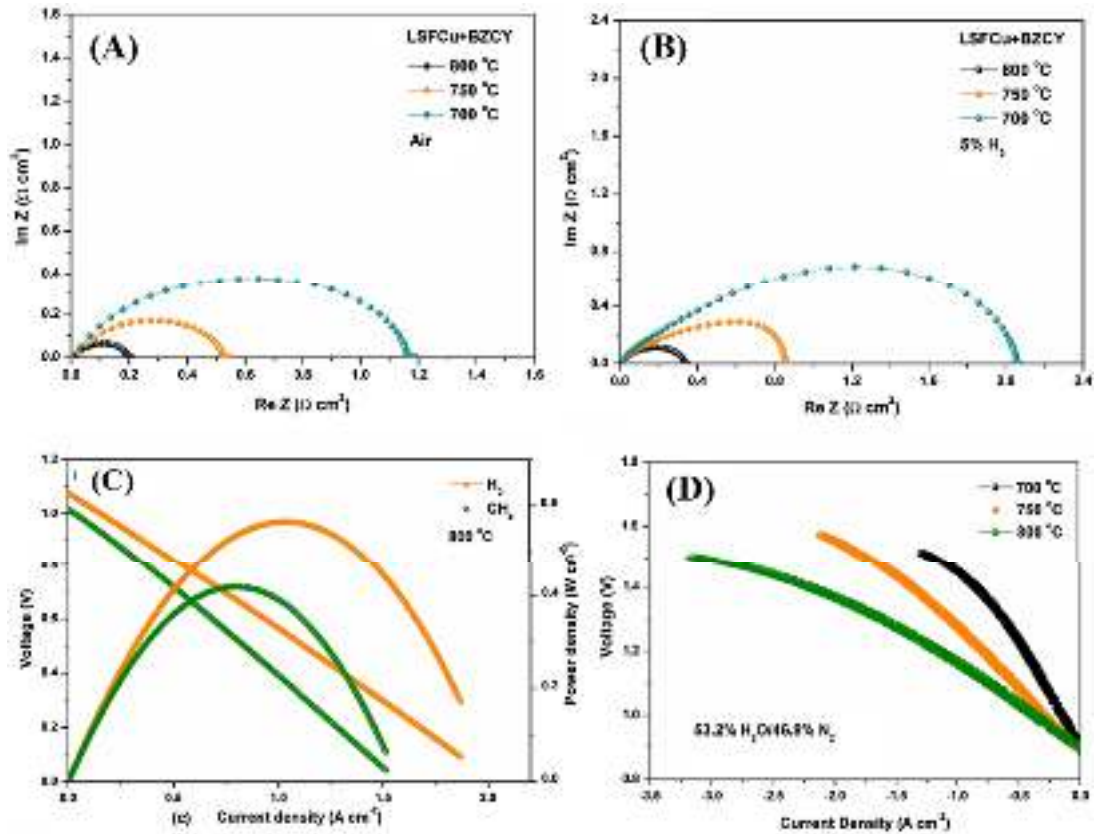


Figure 11. Electrochemical performance of LSFCu symmetrical electrode. (A) Impedance of LSFCu in air. (B) Impedance of LSFCu in 5% H_2 . (C) Cell voltages and power densities as a function of current density of LSFCu symmetrical electrode measured in FC mode using H_2 and CH_4 as fuels. (D) Cell voltages as a function of current density of LSFCu symmetrical electrode measured in EC mode under 53.2% $\text{H}_2\text{O}/46.8\% \text{N}_2$.¹⁴³ Copyright 2020, The ELSEVIER.

Fuel-assisted SSOECs and other applications based on SSOECs

CH_4 has been reported to assist the production of CO on CO_2 electrolysis cells with a dramatically decreased electric input, called partial oxidation of methane.¹⁴⁷⁻¹⁴⁸ It can also be applied for the electrochemical conversion of methane to ethylene in a solid oxide electrolyzer.¹⁴⁹ Therefore, this method was also used in SSOEC. Vasileios Kyriakou et al. reported a low-substitution rhodium-titanate perovskite

(La_{0.43}Ca_{0.37}Rh_{0.06}Ti_{0.94}O₃) electrode for the process, capable of exsolving high Rh nanoparticle populations, and assembled in a SSOC configuration.¹⁵⁰ By introducing dry methane to the anode compartment, the demand for electricity is significantly reduced, even allowing syngas and electricity cogeneration. In order to provide further insight into the role of Rh nanoparticles in methane-to-syngas conversion, they adjusted their size and population by altering the reduction temperature of the perovskite. The results exemplify how the exsolution concept can be used to make efficient use of noble metal to activate low-reactivity greenhouse gas in challenging energy-related applications. Partial oxidation of methane (POM), combined with SOEC technology, gets a promising prospect from this perspective.

As major air pollutants, nitrogen oxides (NO_x) can cause numerous environmental problems such as photochemical smog, acid rain and ozone depletion.¹⁵¹ NO_x is also detrimental to human health, which can gravely destroy the respiratory system.¹⁵² Therefore, curbing NO_x pollution has been a universal issue and various NO_x removal technologies have been developed.¹⁵³⁻¹⁵⁴ SSOEC with LSM/GDC electrode was adopted to electrochemical catalytic reduction of NO.¹⁵⁵ BaO and Pt were infiltrated to electrodes in order to further improve the catalytic activity. The results show that the cell has a certain catalytic activity for the electrochemical catalytic reduction of NO_x with propylene. Pt infiltration promotes the selective reduction of NO_x but BaO infiltration lowered the NO conversion due to the active sites on LSM are blocked. When a voltage was applied to the cell with BaO infiltration electrodes, the conversion of NO increases when there is no propylene and 10% O₂ in the feed gas. In the BaO

infiltration electrode, the addition of propylene did not increase the conversion rate of NO. When Pt is co-infiltrated with BaO, the catalytic activity to reduce NO is enhanced. However, when voltage was applied, almost no effect was found. In addition, when cells are infiltrated by Pt, the electrochemical promotion of CO₂ production is observed. The symmetric cell using LSCM-SDC composite electrode was also designed to remove nitric oxide (NO).¹⁵⁶ The results show that adding an appropriate amount of SDC to the LSCM electrode can improve the cell performance due to the expansion of the three-phase boundary (TPB). The electrode with an SDC of 30 wt.% has the highest NO conversion rate of 69.2% at 750 °C, and the lowest polarization resistance at 1000 ppm NO. Cathodic polarization activates the cathode due to the reduction of Cr/Mn ions, more surface oxygen vacancies and the exsolution of Cr metal. Cells have good tolerance to H₂O, CO₂ and SO₂, but excess O₂ shows a higher activity affinity than NO. The NO conversion decreased sharply when 5% O₂ was introduced as shown in **Figure 12 (A)**. However, the introduction of 5% H₂O even has a positive effect on the NO conversion as shown in **Figure 12 (B)**. Adding 5%CO₂ and 250 ppm SO₂ has slight influence on the NO conversion as shown in **Figure 12 (C, D)**. Moreover, both current density and NO conversion increased by increasing voltage as shown in **Figure 12 (E)**. Single cell stability and flexible working methods have also been demonstrated by alternating DC voltage of ± 2.4 V as shown in **Figure 12 (F)**. The performance keeps stable and it indicates that the symmetrical cells had reversible redox properties. In addition, the mechanism of NO adsorption on the LSCM surface is clarified through density functional theory (DFT) calculations.

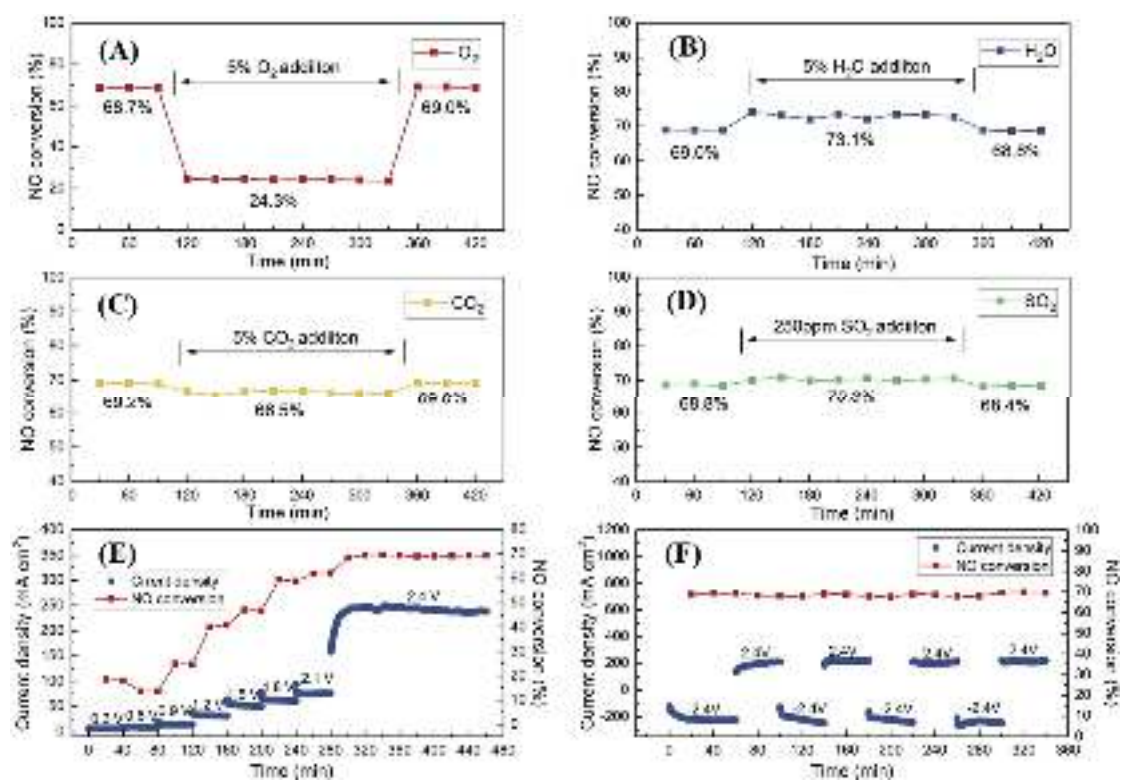


Figure 12. Effects of (A) 5% O₂, (B) 5% H₂O, (C) 5% CO₂ and (D) 250 ppm SO₂ additions on the NO conversions of LSCM-SDC30 under 2.4 V voltage in 1000 ppm NO at 750 °C. Current densities and NO conversions at (E) various voltages and (F) alternating DC voltages of ±2.4 V as the function of operating time. ¹⁵⁶ Copyright 2020, The ELSEVIER.

Ba_{0.5}Sr_{0.5}Co_{0.8}Fe_{0.2}O_{3-δ} (BSCF) powder was prepared by solid-state reaction method. A symmetric cell with SDC as electrolyte and BSCF as electrode was established as an electrochemical reactor for reducing NO_x. In the electrochemical reduction process, NO_x is reduced at the cathode and O₂ is evolved at the anode. ^[157] In order to investigate the NO_x reduction performance of the electrode, the impedance of the symmetric cell in different atmospheres was analyzed. In a symmetrical cell, two different conversion modes are used: dual-chamber and single-chamber. The results suggest that the double-chamber denitrification performance is better, while the single-

chamber structure is simple and has other advantages. The preliminary results of the stability of a single-chamber symmetrical cell indicate that BSCF is the most reliable for reducing nitric oxide in a symmetrical cell. In addition, symmetrical protonic ceramic cells are therefore suggested as hydrogen pumps.¹⁵⁸ Nanoporous Ni-cermet shows high levels of activity for H₂ oxidation and evolution. Excellent H₂ flux of 9.4–15.8 mL·cm⁻²·min⁻¹ is achieved at 350–500 °C.

OUTLOOK

It is important for SSOECs to analysis what actually hindered its development. The challenges and possible future research directions have been listed in **Figure 13**. It mainly including enhancing cell performance, solving cell degradation, clearing reaction mechanism and developing potential application.

Enhancing performance

Despite recent advancements, the SSOECs electrochemical performance is still lower than the traditional anode-supported SOEC. A main reason for this is due to the thick electrolyte supported (usually >300 μm) cell structure. Reducing the thickness of the electrolyte is an effective way to boost efficiency, but it cannot be too small as it makes the cell fragile. Another effective approach is to develop electrolyte materials with superior ionic conductivity such as Bi₂O₃ base electrolyte material. Bi₂O₃ in a fluorite structure (δ-Bi₂O₃) with the highest oxygen ionic conductivity due to a high concentration of oxygen vacancies (around 0.25) and a high anion mobility.¹⁵⁹ Er₂O₃, Dy₂O₃, Gd₂O₃, WO₃ doped or Co doped Bi₂O₃ system were investigated which can display an oxygen ion conductivity of 0.1 S·cm⁻¹ at 500 °C.¹⁶⁰⁻¹⁶¹ It is the highest

conductivity values reported in this temperature regime. These types of materials have achieved excellent electrochemical efficiency, as the conventional SOFC electrolyte. ^[162] However, it has not yet been reported in the SSOEC field. It is, therefore, an electrolyte material of SSOEC with great potential for development. Furthermore, it should be noted that Bi_2O_3 is easy to decompose to metal Bi at low oxygen partial pressure which needs to be resolved in future research. ¹⁶³

To further enhance the SSOEC's efficiency, an exceptional electrode material needs to be developed. Doping, infiltration, in-situ exsolved nanoparticles methods etc. can be used to enhance the electrocatalytic activity. Among them, in situ exsolution is a promising method. There are also studies on applying this method to SSOEC electrodes. Moreover, if the infiltration and in situ exsolution are combined, the exsolution of smaller metal particles on the surface of the nanoelectrode particles obtained by the infiltration method may further improve the performance of the electrode material. However, how to optimize the nanoparticle composition (metal element, alloy) and particle size is still a challenge. Besides, the nano-electrode particles have a tendency to agglomerate and grow up during the long-term operation. Therefore, the delicate balance between electrochemical performance and good stability needs to be further studied. The use of techniques that allow a precise control of the microstructure, e.g. using PMMA microspheres as template, can certainly lead to improving performance. ¹⁶⁴ Moreover, composite optimization via the introduction of other additives or improved grading could also produce better results, and further research is much needed to increase cell efficacy.

As mentioned earlier, SSOECs based on a ceramic proton conductor, or H-SSOEC, have remarkable advantages over SOECs based on an oxygen ion-conducting electrolyte (O-SOEC) for operation at low temperatures. However, relatively little research is being done on H-SSOEC, and additional efforts can be placed in future research to develop new electrodes for proton conductor cells. Double perovskite material has a high oxygen diffusion coefficient and oxygen surface conversion coefficient. Compared to the cathode material of simple perovskite structure, this kind of material exhibits superior thermal stability and thermal expansion coefficient. Moreover, these new cathode materials have high electronic conductivity and relatively low interface impedance. However, the time spent researching these materials is relatively short, and further research is necessary to improve the performance of these materials to a greater extent.

In the first part of the electrode as we mentioned above, the connecting material can be applied as the SSOEC electrode. If we can improve the electrocatalytic activity of the connecting material through a series of modification methods such as doping, infiltration, in-situ exsolved nanoparticles methods etc. There are only two materials in the entire stack system (electrolyte and functional material).¹⁶⁵ Therefore, such a stack can greatly reduce manufacturing and design costs. In fact, tubular configuration cell does not have the sealing problem compared with the flat-plate configuration cell.¹⁶⁶⁻¹⁶⁷ But there is no report on the corresponding tubular symmetrical cell so far. Therefore, we should also pay more attention to the development of tubular symmetrical cell.

Solving degradation

At present, there are not many studies on the long-term stability of SSOECs. The lifetime of the SSOEC should be at least 40 000 h to maintain its competitiveness in the market, but most of the reported SSOECs only display lifetime of hundreds of hours with evident degradation rates. Significant degradation issues were observed under galvanostatic operating conditions caused by the delamination of the oxygen electrode-electrolyte interface. This is associated with the rise in the internal oxygen pressure near the surface of the oxygen electrode due to the OER.¹⁶⁸ The use of robust and more catalytically active functional layers is put forward as a solution for mitigating the delaminating problem along with the easy-to-integrate in reversible symmetrical cells. Sr segregation and Cr poisoning are also the main causes of electrode performance attenuation. The Sr-free and Cr-free electrode can be adopted to solve this problem; besides, novel core-shell structure can also be used to augment electrode stability. In addition, how to maintain the stability of nanoparticles of in situ exsolution also needs to be studied in future work. Carbon deposition and sulfur poisoning are contributing factors. Meanwhile, switching gas is one of the promising solutions for electrode poisoning.

The mentioned above are all that SOFC and SOEC have encountered some troubles so far, but it is unclear whether there will be other problems when SSOEC is towards commercialization. It is an urgent task that operating SSOEC for a long time (over thousands of hours or even longer), try to combined physiochemical characterization (X-ray Photoelectron Spectroscopy, X-ray diffraction, transmission electron microscopy, and scanning electron microscopy) and electrochemical

characterization (electrochemical impedance spectroscopy (EIS) with distribution of relaxation times (DRT) analysis to find out the degradation reason of the SSOEC during long-term operation.¹⁶⁹ Moreover, in order to determine the application of SSOEC, further studies, including the in-situ regeneration process should be explored. The research of redox behavior is particularly important for SSOEC, but the current research in this area is more of the resultant research after oxidation or reduction, it is necessary to strengthen the in-situ characterization and analysis of the redox transformation process.

Clearing mechanism

The mechanism of the ORR and the OER at the transition metal active sites has not been fully understood yet, but the use of methods such as Density Functional Theory (DFT) has allowed us to gain greater understanding.¹⁷⁰ Additional efforts are needed to clarify several aspects of the electrode-electrolyte interface. In fact, the real advantage of SSOECs is that it can reduce the complexity of electrolyte/electrode interface, which makes it easier to clear reaction mechanism, so we should pay more attention to mechanism researches based on SSOECs and get a deeper understanding of it. At present, the reaction process of CO₂RR, HER, OER, etc. of electrode materials still needs more research, as well as the kinetics and reaction barriers of key elementary steps involved in oxygen/proton/electron transfer.¹⁷¹⁻¹⁷² We can use electrochemical impedance spectroscopy (EIS) and distribution of relaxation times (DRT) analysis by controlling H₂O or CO₂ partial pressure to understand the reaction mechanism of CO₂RR, HER deeply. In addition, in-situ characterizations such as near ambient

pressure X-ray Photoelectron Spectroscopy (NAP-XPS),¹⁷³ in situ X-ray diffraction (In situ XRD),¹⁷⁴ in situ diffuse reflectance infrared Fourier transform spectroscopy (DRIFTS),¹⁷⁵ In situ surface enhanced Raman spectroscopic (SERS) can be used to analysis the elementary processes of the electrode reactions. Methods for gathering information are critical for understanding electrocatalysis research, and more information is required to guide the development of near-ideal catalysts.

Potential application

Fuel assisted CO₂ electrolysis has an upbeat perspective, in addition to methane, if carbon is used directly, the effect may also be appropriate. In addition, the use of SOEC technology is also promising to reform CH₄ for production of ethylene.^[176] There is also a certain possibility of using nitrogen to synthesize ammonia with the help of proton conductor cells. Depending on the operating temperature of the electrolytic cell, the combined hydrogen production system of solar energy and the electrolytic cell is studied, and the heat energy and electrical energy required for the hydrogen production process is provided by solar energy. Coupling hydrogen production technology with solar thermal and photoelectric technology could open up new application areas of solar energy.¹⁷⁷⁻¹⁷⁸ Moreover, according to the development trend of SOFC, SOEC will also be operated at medium and low temperatures in order to avoid problems with sealing and material selection. Therefore, it is necessary to develop electrolyte and electrode materials with excellent performance at low and medium temperatures.



Figure 13. Outlook for target SSOECs.

CONCLUSION

Symmetrical solid oxide electrolysis cells using the same electrode materials as both the anode and cathode have attracted lots of attention, Owing to their simple fabrication process, low cost and more convenient. In this review, we summarized the recent progress on developing electrolytes, electrodes for SSOECs, discussing their development history and fundamental mechanisms. Then spotlight examples where fuel-assisted SSOECs to decrease the over potential and other applications based on SSOECs. The outlook for enhancing performance, solving degradation, clearing mechanism and potential application has been demonstrated. To some extent, providing critical insights and useful guidelines for knowledge-based rational design of better electrodes for commercially viable SSOECs. Despite SSOEC possess many advantages, commercialization still needs a long way to go. The key lies in the need to develop high-performance electrolyte and electrode materials, and expand other applications of

SSOEC. It requires the joint efforts of researchers in all fields. We believe that SSOEC technology can benefit all mankind as soon as possible due to their high efficiency and environmentally friendly features.

ACKNOWLEDGMENTS

We gratefully appreciate for financial support from National Key Research & Development Project (2020YFB1506304, 2017YFE0129300), National Natural Science Foundation of China (52072135, 52002121), China Scholarship Council (201806160178), Fundamental Research Funds for the Central Universities (2021QN1111), MOE Key Laboratory for the Green Preparation and Application of Functional Materials, Jiangsu Key Laboratory of Coal-based Greenhouse Gas Control and Utilization (2020KF04).

AUTHOR CONTRIBUTIONS

Yunfeng Tian: Conceptualization, Investigation, Methodology, Writing - Original Draft. **Nalluri Abhishek:** Investigation, Formal analysis. **Caichen Yang:** Investigation, Validation. **Rui Yang:** Investigation, Data Curation. **Choi Sihyuk:** Investigation, Data Curation. **Bo Chi:** Supervision, Data Curation, Review & Editing. **Jian Pu:** Resources, Investigation. **Yihan Ling:** Data Curation, Review & Editing. **Guntae Kim:** Supervision, Review & Editing. **John T.S. Irvine:** Resources, Funding acquisition.

DECLARATION OF INTERESTS

The authors declare no competing financial interest.

REFERENCES

1. Zaman, K.; Abd-el Moemen, M. (2017). Energy consumption, carbon dioxide emissions and economic development: evaluating alternative and plausible environmental hypothesis for sustainable growth. *Renew. Sust. Energy. Rev.* *74*, 1119-1130.
2. Foster, G. L.; Royer, D. L.; Lunt, D. J. (2017). Future climate forcing potentially without precedent in the last 420 million years. *Nat. Commun.* *8*, 14845.
3. Li, X.; Xiong, S.; Li, Z.; Zhou, M.; Li, H. (2019). Variation of global fossil-energy carbon footprints based on regional net primary productivity and the gravity model. *J. clean. prod.* *213*, 225-241.
4. Wang, S.; Li, G.; Fang, C. (2018). Urbanization, economic growth, energy consumption, and CO₂ emissions: Empirical evidence from countries with different income levels. *Renew. Sust. Energy. Rev.* *81*, 2144-2159.
5. Hansen, K.; Mathiesen, B. V.; Skov, I. R. (2019). Full energy system transition towards 100% renewable energy in Germany in 2050. *Renew. Sust. Energy. Rev.* *102*, 1-13.
6. Gielen, D.; Boshell, F.; Saygin, D.; Bazilian, M. D.; Wagner, N.; Gorini, R. (2019). The role of renewable energy in the global energy transformation. *Energy Strategy Rev.* *24*, 38-50.
7. Friebe, C.; Lex-Balducci, A.; Schubert, U. S. (2019). Sustainable Energy Storage: Recent Trends and Developments toward Fully Organic Batteries. *ChemSusChem.* *12*, 4093-4115.
8. Grim, R. G.; Huang, Z.; Guarnieri, M. T.; Ferrell, J. R.; Tao, L.; Schaidle, J. A. (2020). Transforming the carbon economy: challenges and opportunities in the convergence of low-cost electricity and reductive CO₂ utilization. *Energy Environ. Sci.* *13*, 472-494.
9. Wang, R.; Mujahid, M.; Duan, Y.; Wang, Z. K.; Xue, J.; Yang, Y. (2019). A review of perovskites solar cell stability. *Adv. Funct. Mater.* *29*, 1808843.
10. Rana, M.; Ahad, S. A.; Li, M.; Luo, B.; Wang, L.; Gentle, I.; Knibbe, R. (2019). Review on areal capacities and long-term cycling performances of lithium sulfur battery

at high sulfur loading. *Energy Storage Mater.* *18*, 289-310.

11. Wang, Z.; Li, C.; Domen, K. (2019). Recent developments in heterogeneous photocatalysts for solar-driven overall water splitting. *Chem. Soc. Rev.* *48*, 2109-2125.
12. Zhang, G.; Liu, G.; Wang, L.; Irvine, J. T. (2016). Inorganic perovskite photocatalysts for solar energy utilization. *Chem. Soc. Rev.* *45*, 5951-5984.
13. Ding, H.; Wu, W.; Jiang, C.; Ding, Y.; Bian, W.; Hu, B.; Singh, P.; Orme, C. J.; Wang, L.; Zhang, Y. (2020). Self-sustainable protonic ceramic electrochemical cells using a triple conducting electrode for hydrogen and power production. *Nat. Commun.* *11*, 1-11.
14. López Fernández, E.; Gil-Rostra, J.; Espinos, J. P.; Gonzalez-Elipe, A. R.; de Lucas-Consuegra, A.; Yubero, F. (2020). Chemistry and Electrocatalytic Activity of Nanostructured Nickel Electrodes for Water Electrolysis. *ACS Catal.* *10*, 6159–6170.
15. Aftab, W.; Mahmood, A.; Guo, W.; Yousaf, M.; Tabassum, H.; Huang, X.; Liang, Z.; Cao, A.; Zou, R. (2019). Polyurethane-based flexible and conductive phase change composites for energy conversion and storage. *Energy Storage Mater.* *20*, 401-409.
16. Ebbesen, S. D.; Jensen, S. H.; Hauch, A.; Mogensen, M. B. (2014). High temperature electrolysis in alkaline cells, solid proton conducting cells, and solid oxide cells. *Chem. Rev.* *114*, 10697-10734.
17. Panda, C.; Menezes, P. W.; Zheng, M.; Orthmann, S.; Driess, M. (2019). In Situ Formation of Nanostructured Core–Shell Cu_3N – CuO to Promote Alkaline Water Electrolysis. *ACS Energy Lett.* *4*, 747-754.
18. Lei, Z.; Wang, T.; Zhao, B.; Cai, W.; Liu, Y.; Jiao, S.; Li, Q.; Cao, R.; Liu, M. (2020). Recent Progress in Electrocatalysts for Acidic Water Oxidation. *Adv. Energy Mater.* 2000478.
19. Liu, Q.; Yang, C.; Dong, X.; Chen, F. (2010). Perovskite $\text{Sr}_2\text{Fe}_{1.5}\text{Mo}_{0.5}\text{O}_{6-\delta}$ as electrode materials for symmetrical solid oxide electrolysis cells. *Int. J. Hydrogen Energy.* *35*, 10039-10044.
20. Phillips, R.; Edwards, A.; Rome, B.; Jones, D. R.; Dunnill, C. W. (2017). Minimising the ohmic resistance of an alkaline electrolysis cell through effective cell design. *Int. J. Hydrogen Energy.* *42*, 23986-23994.

21. Gong, M.; Wang, D.-Y.; Chen, C.-C.; Hwang, B.-J.; Dai, H. (2016). A mini review on nickel-based electrocatalysts for alkaline hydrogen evolution reaction. *Nano Res.* *9*, 28-46.
22. Phillips, R.; Dunnill, C. W. (2016). Zero gap alkaline electrolysis cell design for renewable energy storage as hydrogen gas. *RSC Adv.* *6*, 100643-100651.
23. Siracusano, S.; Trocino, S.; Briguglio, N.; Baglio, V.; Aricò, A. S. (2018). Electrochemical impedance spectroscopy as a diagnostic tool in polymer electrolyte membrane electrolysis. *Materials* *11*, 1368.
24. Briguglio, N.; Siracusano, S.; Bonura, G.; Sebastián, D.; Aricò, A. S. (2019). Flammability reduction in a pressurised water electrolyser based on a thin polymer electrolyte membrane through a Pt-alloy catalytic approach. *Appl. Catal. B-Environ.* *246*, 254-265.
25. Khatib, F.; Wilberforce, T.; Ijaodola, O.; Ogungbemi, E.; El-Hassan, Z.; Durrant, A.; Thompson, J.; Olabi, A. (2019). Material degradation of components in polymer electrolyte membrane (PEM) electrolytic cell and mitigation mechanisms: A review. *Renew. Sust. Energy. Rev.* *111*, 1-14.
26. Lin, L.; Chen, S.; Quan, J.; Liao, S.; Luo, Y.; Chen, C.; Au, C.-T.; Shi, Y.; Jiang, L. (2020). Geometric synergy of Steam/Carbon dioxide Co-electrolysis and methanation in a tubular solid oxide Electrolysis cell for direct Power-to-Methane. *Energy Conver. Manage.* *208*, 112570.
27. Kim, J.; Jun, A.; Gwon, O.; Yoo, S.; Liu, M.; Shin, J.; Lim, T.-H.; Kim, G. (2018). Hybrid-solid oxide electrolysis cell: A new strategy for efficient hydrogen production. *Nano Energy* *44*, 121-126.
28. Song, Y.; Zhang, X.; Xie, K.; Wang, G.; Bao, X. (2019). High-Temperature CO₂ Electrolysis in Solid Oxide Electrolysis Cells: Developments, Challenges, and Prospects. *Adv. Mater.* *31*, 1902033.
29. Zheng, Y.; Wang, J.; Yu, B.; Zhang, W.; Chen, J.; Qiao, J.; Zhang, J. (2017). A review of high temperature co-electrolysis of H₂O and CO₂ to produce sustainable fuels using solid oxide electrolysis cells (SOECs): advanced materials and technology. *Chem. Soc. Rev.* *46*, 1427-1463.

30. Tong, X.; Ovtar, S.; Brodersen, K.; Hendriksen, P. V.; Chen, M. (2019). A $4 \times 4 \text{ cm}^2$ Nanoengineered Solid Oxide Electrolysis Cell for Efficient and Durable Hydrogen Production. *ACS Appl. Mater. Inter.* *11*, 25996-26004.
31. Ni, M.; Leung, M. K.; Leung, D. Y. (2008). Technological development of hydrogen production by solid oxide electrolyzer cell (SOEC). *Int. J. Hydrogen Energy.* *33*, 2337-2354.
32. Moçoteguy, P.; Brisse, A. (2013). A review and comprehensive analysis of degradation mechanisms of solid oxide electrolysis cells. *Int. J. Hydrogen Energy.* *38*, 15887-15902.
33. Zhang, X.; Song, Y.; Wang, G.; Bao, X. (2017). Co-electrolysis of CO_2 and H_2O in high-temperature solid oxide electrolysis cells: Recent advance in cathodes. *J. Energy Chem.* *26*, 839-853.
34. Zhou, Y.; Lin, L.; Song, Y.; Zhang, X.; Lv, H.; Liu, Q.; Zhou, Z.; Ta, N.; Wang, G.; Bao, X. (2020). Pd single site-anchored perovskite cathode for CO_2 electrolysis in solid oxide electrolysis cells. *Nano Energy* *71*, 104598.
35. Jun, A.; Kim, J.; Shin, J.; Kim, G. (2016). Achieving High Efficiency and Eliminating Degradation in Solid Oxide Electrochemical Cells Using High Oxygen-Capacity Perovskite. *Angew. Chem. Int. Ed.* *55*, 12512-12515.
36. Fan, L.; Zhu, B.; Su, P.-C.; He, C. (2018). Nanomaterials and technologies for low temperature solid oxide fuel cells: recent advances, challenges and opportunities. *Nano Energy* *45*, 148-176.
37. Zhao, C.; Li, Y.; Zhang, W.; Zheng, Y.; Lou, X.; Yu, B.; Chen, J.; Chen, Y.; Liu, M.; Wang, J. (2020). Heterointerface engineering for enhancing the electrochemical performance of solid oxide cells. *Energy Environ. Sci.* *13*, 53-85
38. Shin, E.-C.; Ma, J.; Ahn, P.-A.; Seo, H.-H.; Nguyen, D. T.; Lee, J. S. (2016). Deconvolution of four transmission-line-model impedances in Ni-YSZ/YSZ/LSM solid oxide cells and mechanistic insights. *Electrochim. Acta.* *188*, 240-253.
39. Tian, Y.; Liu, Y.; Wang, W.; Jia, L.; Pu, J.; Chi, B.; Li, J. (2020). High performance and stability of double perovskite-type oxide $\text{NdBa}_{0.5}\text{Ca}_{0.5}\text{Co}_{1.5}\text{Fe}_{0.5}\text{O}_{5+\delta}$ as an oxygen electrode for reversible solid oxide electrochemical cell. *J. Energy Chem.* *43*, 108-115.

40. Dong, D.; Xu, S.; Shao, X.; Hucker, L.; Marin, J.; Pham, T.; Xie, K.; Ye, Z.; Yang, P.; Yu, L. (2017). Hierarchically ordered porous Ni-based cathode-supported solid oxide electrolysis cells for stable CO₂ electrolysis without safe gas. *J. Mater. Chem. A*. *5*, 24098-24102.
41. Sreedhar, I.; Agarwal, B.; Goyal, P.; Singh, S. A. (2019). Recent advances in material and performance aspects of solid oxide fuel cells. *Electroanal. Chem.* 113315.
42. Zhang, J.; Lei, L.; Li, H.; Chen, F.; Han, M. (2021). A practical approach for identifying various polarization behaviors of redox-stable electrodes in symmetrical solid oxide fuel cells. *Electrochim. Acta.* *384*, 138340.
43. Weissbart, J.; Smart, W.; Wydeven, T. (1969). Oxygen reclamation from carbon dioxide using a solid oxide electrolyte. *Aerosp. med.* *40*, 136-140.
44. Isenberg, A. (1981). Energy conversion via solid oxide electrolyte electrochemical cells at high temperatures. *Solid State Ionics* *3*, 431-437.
45. Hauch, A.; Ebbesen, S. D.; Jensen, S. H.; Mogensen, M. (2008). Highly efficient high temperature electrolysis. *J. Mater. Chem.* *18*, 2331-2340.
46. Badding, M. E.; Brown, J. L.; Ketcham, T. D.; Julien, D. J. S.; Wusirika, R. R. (2003). High performance solid electrolyte fuel cells. Google Patents.
47. Su, C.; Wang, W.; Liu, M.; Tadé, M. O.; Shao, Z. (2015). Progress and prospects in symmetrical solid oxide fuel cells with two identical electrodes. *Adv. Energy Mater.* *5*, 1500188.
48. Zhang, Y.; Zhao, H.; Du, Z.; Świerczek, K.; Li, Y. (2019). High-Performance SmBaMn₂O_{5+δ} Electrode for Symmetrical Solid Oxide Fuel Cell. *Chem. Mater.* *31*, 3784-3793.
49. Fan, W.; Sun, Z.; Bai, Y.; Wu, K.; Cheng, Y. (2019). Highly Stable and Efficient Perovskite Ferrite Electrode for Symmetrical Solid Oxide Fuel Cells. *ACS Appl. Mater. Inter.* *11*, 23168-23179.
50. Gu, Y.; Zhang, Y.; Zheng, Y.; Chen, H.; Ge, L.; Guo, L. (2019). PrBaMn₂O_{5+δ} with praseodymium oxide nano-catalyst as electrode for symmetrical solid oxide fuel cells. *Appl. Catal. B-Environ.* *257*, 117868.
51. Bian, L.; Duan, C.; Wang, L.; O'Hayre, R.; Cheng, J.; Chou, K.-C. (2017). Ce-

doped $\text{La}_{0.7}\text{Sr}_{0.3}\text{Fe}_{0.9}\text{Ni}_{0.1}\text{O}_{3-\delta}$ as symmetrical electrodes for high performance direct hydrocarbon solid oxide fuel cells. *J. Mater. Chem. A.* *5*, 15253-15259.

52. Zhou, J.; Shin, T.-H.; Ni, C.; Chen, G.; Wu, K.; Cheng, Y.; Irvine, J. T. (2016). In situ growth of nanoparticles in layered perovskite $\text{La}_{0.8}\text{Sr}_{1.2}\text{Fe}_{0.9}\text{Co}_{0.1}\text{O}_{4-\delta}$ as an active and stable electrode for symmetrical solid oxide fuel cells. *Chem. Mater.* *28*, 2981-2993.

53. Liu, Q.; Dong, X.; Xiao, G.; Zhao, F.; Chen, F. (2010). A novel electrode material for symmetrical SOFCs. *Adv. Mater.* *22*, 5478-5482.

54. Bi, L.; Shafi, S. P.; Da'as, E. H.; Traversa, E. (2018). Tailoring the cathode-electrolyte interface with nanoparticles for boosting the solid oxide fuel cell performance of chemically stable proton-conducting electrolytes. *Small* *14*, 1801231.

55. Huan, D.; Shi, N.; Zhang, L.; Tan, W.; Xie, Y.; Wang, W.; Xia, C.; Peng, R.; Lu, Y. (2018). New, efficient, and reliable air electrode material for proton-conducting reversible solid oxide cells. *ACS Appl. Mater. Inter.* *10*, 1761-1770.

56. Jin, C.; Yang, C.; Chen, F. (2011). Characteristics of the Hydrogen Electrode in High Temperature Steam Electrolysis Process. *J. Electrochem. Soc.* *158*, B1217-B1223.

57. Kleiminger, L.; Li, T.; Li, K.; Kelsall, G. (2015). Syngas (CO-H_2) production using high temperature micro-tubular solid oxide electrolyzers. *Electrochim. Acta.* *179*, 565-577.

58. Singh, B.; Ghosh, S.; Aich, S.; Roy, B. (2017). Low temperature solid oxide electrolytes (LT-SOE): A review. *J. Power Sources* *339*, 103-135.

59. Xu, S.; Li, S.; Yao, W.; Dong, D.; Xie, K. (2013). Direct electrolysis of CO_2 using an oxygen-ion conducting solid oxide electrolyzer based on $\text{La}_{0.75}\text{Sr}_{0.25}\text{Cr}_{0.5}\text{Mn}_{0.5}\text{O}_{3-\delta}$ electrode. *J. Power Sources* *230*, 115-121.

60. Xu, J.; Zhou, X.; Cheng, J.; Pan, L.; Wu, M.; Dong, X.; Sun, K. (2017). Electrochemical performance of highly active ceramic symmetrical electrode $\text{La}_{0.3}\text{Sr}_{0.7}\text{Ti}_{0.3}\text{Fe}_{0.7}\text{O}_{3-\delta}\text{-CeO}_2$ for reversible solid oxide cells. *Electrochim. Acta.* *257*, 64-72.

61. Kostogloudis, G. C.; Tsiniarakis, G.; Ftikos, C. (2000). Chemical reactivity of perovskite oxide SOFC cathodes and yttria stabilized zirconia. *Solid State Ionics* *135*, 529-535.

62. Adijanto, L.; Kungas, R.; Bidrawn, F.; Gorte, R.; Vohs, J. (2011). Stability and performance of infiltrated $\text{La}_{0.8}\text{Sr}_{0.2}\text{Co}_x\text{Fe}_{1-x}\text{O}_3$ electrodes with and without $\text{Sm}_{0.2}\text{Ce}_{0.8}\text{O}_{1.9}$ interlayers. *J. Power Sources* 196, 5797-5802.
63. Yamamoto, O. (2010). Low temperature electrolytes and catalysts. *Handbook of fuel cells*.
64. Laguna-Bercero, M.; Skinner, S.; Kilner, J. (2009). Performance of solid oxide electrolysis cells based on scandia stabilised zirconia. *J. Power Sources* 192 (1), 126-131.
65. Arunkumar, P.; Meena, M.; Babu, K. S. (2012). A review on cerium oxide-based electrolytes for ITSOFC. *Nanomaterials and Energy* 1, 288-305.
66. Sumi, H.; Suda, E.; Mori, M. (2017). Blocking layer for prevention of current leakage for reversible solid oxide fuel cells and electrolysis cells with ceria-based electrolyte. *Int. J. Hydrogen Energy*. 42, 4449-4455.
67. Stijepovic, I.; Darbandi, A. J.; Srdic, V. V. (2013). Conductivity of Co and Ni doped lanthanum-gallate synthesized by citrate sol-gel method. *Ceram. Int.* 39, 1495-1502.
68. Basbus, J. F.; Arce, M. D.; Napolitano, F. R.; Troiani, H. E.; Alonso, J. A.; Saleta, M. E.; González, M. A.; Cuello, G. J.; Fernández-Díaz, M. a. T.; Sainz, M. P. (2020). Revisiting the Crystal Structure of $\text{BaCe}_{0.4}\text{Zr}_{0.4}\text{Y}_{0.2}\text{O}_{3-\delta}$ Proton Conducting Perovskite and Its Correlation with Transport Properties. *ACS Appl. Energy Mater.* 3, 2881-2892.
69. Pergolesi, D.; Fabbri, E.; D'Epifanio, A.; Di Bartolomeo, E.; Tebano, A.; Sanna, S.; Licoccia, S.; Balestrino, G.; Traversa, E. (2010). High proton conduction in grain-boundary-free yttrium-doped barium zirconate films grown by pulsed laser deposition. *Nat. Mater.* 9, 846-850.
70. Iwahara, H. (1988). High temperature proton conducting oxides and their applications to solid electrolyte fuel cells and steam electrolyzer for hydrogen production. *Solid State Ionics* 28, 573-578.
71. Bausá, N.; Escolástico, S.; Serra, J. M. (2019). Direct CO_2 conversion to syngas in a $\text{BaCe}_{0.2}\text{Zr}_{0.7}\text{Y}_{0.1}\text{O}_{3-\delta}$ -based proton-conducting electrolysis cell. *J CO₂ Util.* 34, 231-238.
72. Gan, L.; Ye, L.; Wang, S.; Liu, M.; Tao, S.; Xie, K. (2016). Demonstration of direct

conversion of CO₂/H₂O into syngas in a symmetrical proton-conducting solid oxide electrolyzer. *Int. J. Hydrogen Energy*. *41*, 1170-1175.

73. Yang, L.; Wang, S.; Blinn, K.; Liu, M.; Liu, Z.; Cheng, Z.; Liu, M. (2009). Enhanced sulfur and coking tolerance of a mixed ion conductor for SOFCs: BaZr_{0.1}Ce_{0.7}Y_{0.2-x}Yb_xO_{3-δ}. *Science* *326*, 126-129.

74. Lei, L.; Zhang, J.; Yuan, Z.; Liu, J.; Ni, M.; Chen, F. (2019). Progress Report on Proton Conducting Solid Oxide Electrolysis Cells. *Adv. Funct. Mater.* *29*, 1903805.

75. Duan, C.; Kee, R.; Zhu, H.; Sullivan, N.; Zhu, L.; Bian, L.; Jennings, D.; O'Hayre, R. (2019). Highly efficient reversible protonic ceramic electrochemical cells for power generation and fuel production. *Nat. Energy* *4*, 230-240.

76. Xu, J.; Chen, C.; Han, Z.; Yang, Y.; Li, J.; Deng, Q. (2019). Recent Advances in Oxygen Electrocatalysts Based on Perovskite Oxides. *Nanomaterials* *9*, 1161.

77. Pena, M.; Fierro, J. (2001). Chemical structures and performance of perovskite oxides. *Chem. Rev.* *101*, 1981-2018.

78. Grabowska, E. (2016). Selected perovskite oxides: characterization, preparation and photocatalytic properties—a review. *Appl. Catal. B-Environ.* *186*, 97-126.

79. Yan, D.; Li, Y.; Huo, J.; Chen, R.; Dai, L.; Wang, S. (2017). Defect chemistry of nonprecious-metal electrocatalysts for oxygen reactions. *Adv. Mater.* *29*, 1606459.

80. Tao, S.; Irvine, J. T. (2003). A redox-stable efficient anode for solid-oxide fuel cells. *Nat. Mater.* *2*, 320-323.

81. Tao, S.; Irvine, J. T. (2004). Synthesis and Characterization of (La_{0.75}Sr_{0.25})Cr_{0.5}Mn_{0.5}O_{3-δ}, a Redox-Stable, Efficient Perovskite Anode for SOFCs. *J. Electrochem. Soc.* *151*, A252-A259.

82. Ruan, C.; Xie, K.; Yang, L.; Ding, B.; Wu, Y. (2014). Efficient carbon dioxide electrolysis in a symmetric solid oxide electrolyzer based on nanocatalyst-loaded chromate electrodes. *Int. J. Hydrogen Energy*. *39*, 10338-10348.

83. Chen, S.; Xie, K.; Dong, D.; Li, H.; Qin, Q.; Zhang, Y.; Wu, Y. (2015). A composite cathode based on scandium-doped chromate for direct high-temperature steam electrolysis in a symmetric solid oxide electrolyzer. *J. Power Sources* *274*, 718-729.

84. Torrell, M.; García-Rodríguez, S.; Morata, A.; Penelas, G.; Tarancón, A. (2015).

Co-electrolysis of steam and CO₂ in full-ceramic symmetrical SOECs: a strategy for avoiding the use of hydrogen as a safe gas. *Faraday discuss.* *182*, 241-255.

85. Yang, X.; Irvine, J. T. (2008). (La_{0.75}Sr_{0.25})_{0.95}Mn_{0.5}Cr_{0.5}O₃ as the cathode of solid oxide electrolysis cells for high temperature hydrogen production from steam. *J. Mater. Chem.* *18*, 2349-2354.

86. Yokokawa, H.; Sakai, N.; Kawada, T.; Dokiya, M. (1992). Thermodynamic stabilities of perovskite oxides for electrodes and other electrochemical materials. *Solid State Ionics.* *52*, 43-56.

87. Li, J.; Wei, B.; Cao, Z.; Yue, X.; Zhang, Y.; Lü, Z. (2018). Niobium Doped Lanthanum Strontium Ferrite as A Redox-Stable and Sulfur-Tolerant Anode for Solid Oxide Fuel Cells. *ChemSusChem* *11*, 254-263.

88. Zhao, X.-H.; Wang, Y.; Liu, L.-M. (2017). Preparation and Electrochemical Performance of a Novel Perovskite Anode La_{0.9}Ca_{0.1}Fe_{0.9}Nb_{0.1}O_{3-δ} for Solid Oxide Fuel Cells. *J INORG MATE-BEIJING.* *32*, 1188-1194.

89. Lee, K.-J.; Lee, M.-J.; Park, S.-h.; Hwang, H.-J.; Lee, K.-J.; Lee, M.-J.; Park, S.-h.; Hwang, H.-J. (2016). Symmetrical Solid Oxide Electrolyzer Cells (SOECs) with La_{0.6}Sr_{0.4}Co_{0.2}Fe_{0.8}O₃ (LSCF)-Gadolinium Doped Ceria (GDC) Composite Electrodes. *J. Korean. Ceram. Soc.* *53*, 489-493.

90. Guan, F.; Zhang, X.; Song, Y.; Zhou, Y.; Wang, G.; Bao, X. (2018). Effect of Gd_{0.2}Ce_{0.8}O_{1.9} nanoparticles on the oxygen evolution reaction of La_{0.6}Sr_{0.4}Co_{0.2}Fe_{0.8}O_{3-δ} anode in solid oxide electrolysis cell. *Chin. J. Catal.* *39*, 1484-1492.

91. Huang, Z.; Qi, H.; Zhao, Z.; Shang, L.; Tu, B.; Cheng, M. (2019). Efficient CO₂ electroreduction on a solid oxide electrolysis cell with La_{0.6}Sr_{0.4}Co_{0.2}Fe_{0.8}O_{3-δ}-Gd_{0.2}Ce_{0.8}O_{2-δ} infiltrated electrode. *J. Power Sources* *434*, 226730.

92. Kulkarni, A.; Giddey, S.; Badwal, S. (2017). Efficient conversion of CO₂ in solid oxide electrolytic cells with Pd doped perovskite cathode on ceria nanofilm interlayer. *J CO₂ Util.* *17*, 180-187.

93. Yang, Z.; Wang, N.; Ma, C.; Jin, X.; Lei, Z.; Xiong, X.; Peng, S. (2019). Co-electrolysis of H₂O-CO₂ in a solid oxide electrolysis cell with symmetrical La_{0.4}Sr_{0.6}Co_{0.2}Fe_{0.7}Nb_{0.1}O_{3-δ} electrode. *J Electroana. Chem.* *836*, 107-111.

94. Yang, Z.; Ma, C.; Wang, N.; Jin, X.; Jin, C.; Peng, S. (2019). Electrochemical reduction of CO₂ in a symmetrical solid oxide electrolysis cell with La_{0.4}Sr_{0.6}Co_{0.2}Fe_{0.7}Nb_{0.1}O_{3-δ} electrode. *J CO₂ Util.* *33*, 445-451.
95. Laguna-Bercero, M. (2012). Recent advances in high temperature electrolysis using solid oxide fuel cells: A review. *J. Power Sources* *203*, 4-16.
96. Chen, G.; Sunarso, J.; Wang, Y.; Ge, C.; Yang, J.; Liang, F. (2016). Evaluation of A-site deficient Sr_{1-x}Sc_{0.175}Nb_{0.025}Co_{0.8}O_{3-δ} (x= 0, 0.02, 0.05 and 0.1) perovskite cathodes for intermediate-temperature solid oxide fuel cells. *Ceram Int.* *42*, 12894-12900.
97. Cao, Z.; Wei, B.; Miao, J.; Wang, Z.; Lü, Z.; Li, W.; Zhang, Y.; Huang, X.; Zhu, X.; Feng, Q. (2016). Efficient electrolysis of CO₂ in symmetrical solid oxide electrolysis cell with highly active La_{0.3}Sr_{0.7}Fe_{0.7}Ti_{0.3}O₃ electrode material. *Electrochem Commun.* *69*, 80-83.
98. Kumari, N.; Haider, M. A.; Basu, S. (2017). Reduction of CO₂ to CO in presence of H₂ on strontium doped lanthanum manganite cathode in solid oxide electrolysis cell. *J. Chem. Sci.* *129*, 1735-1740.
99. Tian, Y.; Zheng, H.; Zhang, L.; Chi, B.; Pu, J.; Li, J. (2018). Direct electrolysis of CO₂ in symmetrical solid oxide electrolysis cell based on La_{0.6}Sr_{0.4}Fe_{0.8}Ni_{0.2}O_{3-δ} electrode. *J. Electrochem. Soc.* *165*, F17-F23.
100. Tian, Y.; Zhang, L.; Jia, L.; Wang, X.; Yang, J.; Chi, B.; Pu, J.; Li, J. (2019). Novel quasi-symmetrical solid oxide electrolysis cells with in-situ exsolved cathode for CO₂ electrolysis. *J CO₂ Util.* *31*, 43-50.
101. Peng, X.; Tian, Y.; Liu, Y.; Wang, W.; Jia, L.; Pu, J.; Chi, B.; Li, J. (2020). An efficient symmetrical solid oxide electrolysis cell with LSFM-based electrodes for direct electrolysis of pure CO₂. *J CO₂ Util.* *36*, 18-24.
102. Wang, S.; Tsuruta, H.; Asanuma, M.; Ishihara, T. (2015). Ni-Fe-La(Sr)Fe(Mn)O₃ as a new active cermet cathode for intermediate-temperature CO₂ electrolysis using a LaGaO₃-based electrolyte. *Adv. Energy Mater.* *5*, 1401003.
103. Kim, D.; Bliem, R.; Hess, F.; Gallet, J.-J.; Yildiz, B. (2020). Electrochemical polarization dependence of the elastic and electrostatic driving forces to aliovalent

dopant segregation on LaMnO₃. *J. Am. Chem. Soc.* *142*, 3548–3563.

104. Koo, B.; Kim, K.; Kim, J. K.; Kwon, H.; Han, J. W.; Jung, W. (2018). Sr segregation in perovskite oxides: why it happens and how it exists. *Joule* *2*, 1476-1499.

105. Tian, Y.; Zhang, L.; Liu, Y.; Jia, L.; Yang, J.; Chi, B.; Pu, J.; Li, J. (2019). A self-recovering robust electrode for highly efficient CO₂ electrolysis in symmetrical solid oxide electrolysis cells. *J. Mater. Chem. A.* *7*, 6395-6400.

106. Pang, S.; Xu, J.; Su, Y.; Yang, G.; Zhu, M.; Cui, M.; Shen, X.; Chen, C. (2020). The role of A-site cation size mismatch in tune the catalytic activity and durability of double perovskite oxides. *Appl. Catal. B-Environ.* 118868.

107. Chen, Y.; Yoo, S.; Choi, Y.; Kim, J. H.; Ding, Y.; Pei, K.; Murphy, R.; Zhang, Y.; Zhao, B.; Zhang, W. (2018). A highly active, CO₂-tolerant electrode for the oxygen reduction reaction. *Energy Environ. Sci.* *11*, 2458-2466.

108. Hua, B.; Zhang, Y. Q.; Yan, N.; Li, M.; Sun, Y. F.; Chen, J.; Li, J.; Luo, J. L. (2016). The excellence of both worlds: developing effective double perovskite oxide catalyst of oxygen reduction reaction for room and elevated temperature applications. *Adv. Funct. Mater.* *26*, 4106-4112.

109. Wang, Y.; Liu, T.; Fang, S.; Chen, F. (2016). Syngas production on a symmetrical solid oxide H₂O/CO₂ co-electrolysis cell with Sr₂Fe_{1.5}Mo_{0.5}O_{6-δ}-Sm_{0.2}Ce_{0.8}O_{1.9} electrodes. *J. Power Sources* *305*, 240-248.

110. Li, Y.; Zhan, Z.; Xia, C. (2018). Highly efficient electrolysis of pure CO₂ with symmetrical nanostructured perovskite electrodes. *Catal. Sci. Technol.* *8*, 980-984.

111. Hou, S.; Xie, K. (2019). Enhancing the performance of high-temperature H₂O/CO₂ co-electrolysis process on the solid oxide Sr₂Fe_{1.6}Mo_{0.5}O_{6-δ}-SDC/LSGM/Sr₂Fe_{1.5}Mo_{0.5}O_{6-δ}-SDC cell. *Electrochim. Acta* *301*, 63-68.

112. Bernadet, L.; Moncasi, C.; Torrell, M.; Tarancón, A. (2020). High-performing electrolyte-supported symmetrical solid oxide electrolysis cells operating under steam electrolysis and co-electrolysis modes. *Int. J. Hydrogen Energy.* *45*, 14208-14217.

113. Zhou, J.; Xu, L.; Ding, C.; Wei, C.; Tao, Z. (2019). Layered perovskite (PrBa)_{0.95}(Fe_{0.9}Mo_{0.1})₂O_{5+δ} as electrode materials for high-performing symmetrical solid oxide electrolysis cells. *Mater. Lett.* *257*, 126758.

114. Niu, B.; Lu, C.; Yi, W.; Luo, S.; Li, X.; Zhong, X.; Zhao, X.; Xu, B. (2020). In-situ growth of nanoparticles-decorated double perovskite electrode materials for symmetrical solid oxide cells. *Appl. Catal. B-Environ.* 118842.
115. Chen, Y.; Yoo, S.; Choi, Y. M.; Kim, J.; Hyuk; D. (2018). A highly active, CO₂-tolerant electrode for the oxygen reduction reaction. *Energy Environ. Sci.* 11, 2458-2466.
116. Li, M.; Chen, K.; Hua, B.; Luo, J.; Rickard, W. D. A.; Li, J.; Irvine, J. T. S.; Jiang, S. P. (2016). Smart utilization of cobaltite-based double perovskite cathodes on barrier-layer-free zirconia electrolyte of solid oxide fuel cells. *J. Mater. Chem. A.* 4, 19019-19025.
117. Jun, A., Yoo, S.Y., Ju, Y.W., Hyodo, J., Choi, S., Jeong, H. Y., Shin, J., Ishihara, T., Lim, T., Kim, G. (2015). Correlation between fast oxygen kinetics and enhanced performance in Fe doped layered perovskite cathodes for solid oxide fuel cells. *J. Mater. Chem. A.* 3, 15082-15090.
118. Marco, J. F.; Gancedo, J. R.; Gracia, M.; Gautier, J. L.; Ríos, E. I.; Palmer, H. M.; Greaves, C.; Berry, F. J. (2001). Cation distribution and magnetic structure of the ferrimagnetic spinel NiCo₂O₄. *J. Mater. Chem.* 11, 3087-3093.
119. Sonoyama, N.; Kawamura, K.; Yamada, A.; Kanno, R. (2006). Electrochemical luminescence of rare earth metal ion doped MgIn₂O₄ electrodes. *J. Electrochem. Soc.* 153, H45-H50.
120. Stefan, E.; Connor, P. A.; Azad, A. K.; Irvine, J. T. (2014). Structure and properties of MgM_xCr_{2-x}O₄ (M= Li, Mg, Ti, Fe, Cu, Ga) spinels for electrode supports in solid oxide fuel cells. *J. Mater. Chem. A.* 2, 18106-18114.
121. Stefan, E.; Tsekouras, G.; Irvine, J. T. (2013). Development and Performance of MnFeCrO₄-Based Electrodes for Solid Oxide Fuel Cells. *Adv. Energy Mater.* 3, 1454-1462.
122. Zhang, L.; Tian, Y.; Liu, Y.; Jia, L.; Yang, J.; Chi, B.; Pu, J.; Li, J. (2019). Direct Electrolysis of CO₂ in a Symmetrical Solid Oxide Electrolysis Cell with Spinel MnCo₂O₄ as Electrode. *ChemElectroChem* 6, 1359-1364.
123. Duan, N.; Gao, M.; Hua, B.; Li, M.; Chi, B.; Li, J.; Luo, J.-L. (2020). Exploring

Ni (Mn_{1/3}Cr_{2/3})₂O₄ Spinel-Based Electrode for Solid Oxide Cell. *J. Mater. Chem. A*, *8*, 3988-3998.

124. Li, J.; Zhang, Q.; Qiu, P.; Chi, B.; Pu, J.; Li, J. (2017). A CO₂-tolerant La₂NiO_{4+δ}-coated PrBa_{0.5}Sr_{0.5}Co_{1.5}Fe_{0.5}O_{5+δ} cathode for intermediate temperature solid oxide fuel cells. *J. Power Sources* *342*, 623-628.

125. Qiu, P.; Wang, A.; Li, J.; Chi, B.; Pu, J.; Li, J. (2016). Promoted CO₂-poisoning resistance of La_{0.8}Sr_{0.2}MnO_{3-δ}-coated Ba_{0.5}Sr_{0.5}Co_{0.8}Fe_{0.2}O_{3-δ} cathode for intermediate temperature solid oxide fuel cells. *J. Power Sources* *327*, 408-413.

126. Liu, Q.; Dong, X.; Xiao, G.; Zhao, F.; Chen, F. (2010). A novel electrode material for symmetrical SOFCs. *Adv. Mater.* *22*, 5478-82.

127. Li, M.; Hua, B.; Chen, J.; Zhong, Y.; Luo, J.-L. (2019). Charge transfer dynamics in RuO₂/perovskite nanohybrid for enhanced electrocatalysis in solid oxide electrolyzers. *Nano Energy* *57*, 186-194.

128. Zhang, S.-L.; Wang, H.; Lu, M. Y.; Zhang, A.-P.; Mogni, L. V.; Liu, Q.; Li, C.-X.; Li, C.-J.; Barnett, S. A. (2018). Cobalt-substituted SrTi_{0.3}Fe_{0.7}O_{3-δ}: a stable high-performance oxygen electrode material for intermediate-temperature solid oxide electrochemical cells. *Energy Environ. Sci.* *11*, 1870-1879.

129. Molero-Sánchez, B.; Addo, P. K.; Buyukaksoy, A.; Birss, V. (2015). GDC-Infiltrated La_{0.3}Ca_{0.7}Fe_{0.7}Cr_{0.3}O_{3-δ} Symmetrical Oxygen Electrodes for Reversible SOFCs. *ECS Trans.* *66*, 185-193.

130. Molero-Sánchez, B.; Addo, P.; Buyukaksoy, A.; Paulson, S.; Birss, V. (2015). Electrochemistry of La_{0.3}Sr_{0.7}Fe_{0.7}Cr_{0.3}O_{3-δ} as an oxygen and fuel electrode for RSOFCs. *Faraday discuss* *182*, 159-175.

131. Addo, P.; Molero-Sanchez, B.; Chen, M.; Paulson, S.; Birss, V. (2015). CO/CO₂ study of high performance La_{0.3}Sr_{0.7}Fe_{0.7}Cr_{0.3}O_{3-δ} reversible SOFC electrodes. *Fuel Cells* *15*, 689-696.

132. Molero-Sánchez, B.; Morán, E.; Birss, V. (2017). Rapid and Low-Energy Fabrication of Symmetrical Solid Oxide Cells by Microwave Methods. *ACS omega* *2*, 3716-3723.

133. Bian, L.; Duan, C.; Wang, L.; Hou, Y.; Zhu, L.; O'Hayre, R.; Chou, K.-C.

(2018). Highly Efficient, Redox-Stable, $\text{La}_{0.5}\text{Sr}_{0.5}\text{Fe}_{0.9}\text{Nb}_{0.1}\text{O}_{3-\delta}$ Symmetric Electrode for Both Solid-Oxide Fuel Cell and $\text{H}_2\text{O}/\text{CO}_2$ Co-Electrolysis Operation. *J. Electrochem. Soc.* *165*, F981-F986.

134. Kim, S.; Lee, S.; Kim, J.; Shin, J.; Kim, G. (2018). Self-Transforming Configuration Based on Atmospheric-Adaptive Materials for Solid Oxide Cells. *Sci. Rep.* *8*, 1-7.

135. Li, Y.; Zou, S.; Ju, J.; Xia, C. (2018). Characteristics of nano-structured SFM infiltrated onto YSZ backbone for symmetrical and reversible solid oxide cells. *Solid State Ionics* *319*, 98-104.

136. Guo, Y.; Guo, T.; Zhou, S.; Wu, Y.; Chen, H.; Ou, X.; Ling, Y. (2019). Characterization of $\text{Sr}_2\text{Fe}_{1.5}\text{Mo}_{0.5}\text{O}_{6-\delta}\text{-Gd}_{0.1}\text{Ce}_{0.9}\text{O}_{1.95}$ symmetrical electrode for reversible solid oxide cells. *Ceram Int.* *45*, 10969-10975.

137. Carollo, G.; Garbujo, A.; Bedon, A.; Ferri, D.; Natile, M.; Glisenti, A. (2018). Cu/CGO Cermet Based Electrodes for Symmetric and Reversible Solid Oxide Fuel Cells. *Int. J. Hydrogen Energy.* *45*, 13652-13658.

138. Zhou, J.; Wang, N.; Cui, J.; Wang, J.; Yang, J.; Zong, Z.; Zhang, Z.; Chen, Q.; Zheng, X.; Wu, K. (2019). Structural and electrochemical properties of B-site Ru-doped $(\text{La}_{0.8}\text{Sr}_{0.2})_{0.9}\text{Sc}_{0.2}\text{Mn}_{0.8}\text{O}_{3-\delta}$ as symmetrical electrodes for reversible solid oxide cells. *J. Alloy. Compod.* *792*, 1132-1140.

139. Lei, L.; Tao, Z.; Wang, X.; Lemmon, J. P.; Chen, F. (2017). Intermediate-temperature solid oxide electrolysis cells with thin proton-conducting electrolyte and a robust air electrode. *J. Mater. Chem. A.* *5*, 22945-22951.

140. Vøllestad, E.; Strandbakke, R.; Tarach, M.; Catalán-Martínez, D.; Fontaine, M.-L.; Beaff, D.; Clark, D. R.; Serra, J. M.; Norby, T. (2019). Mixed proton and electron conducting double perovskite anodes for stable and efficient tubular proton ceramic electrolyzers. *Nat. Mater.* *18*, 752-759.

141. Pu, T.; Tan, W.; Shi, H.; Na, Y.; Lu, J.; Zhu, B. (2016). Steam/ CO_2 electrolysis in symmetric solid oxide electrolysis cell with barium cerate-carbonate composite electrolyte. *Electrochim. Acta* *190*, 193-198.

142. Tarutin, A.; Lyagaeva, J.; Farlenkov, A.; Plaksin, S.; Vdovin, G.; Demin, A.;

- Medvedev, D. (2019). A reversible protonic ceramic cell with symmetrically designed $\text{Pr}_2\text{NiO}_{4+\delta}$ -based electrodes: fabrication and electrochemical features. *Materials* *12*, 118.
143. Fu, L.; Zhou, J.; Yang, J.; Lian, Z.; Wang, J.; Cheng, Y.; Wu, K. (2020). Exsolution of Cu nanoparticles in $(\text{LaSr})_{0.9}\text{Fe}_{0.9}\text{Cu}_{0.1}\text{O}_4$ Ruddlesden-Popper oxide as symmetrical electrode for solid oxide cells. *Appl. Sur. Sci.* *511*, 145525.
144. Duan, C.; Tong, J.; Shang, M.; Nikodemski, S.; Sanders, M.; Ricote, S.; Almansoori, A.; O'Hayre, R. (2015). Readily processed protonic ceramic fuel cells with high performance at low temperatures. *Science* *349*, 1321-1326.
145. Duan, C.; Kee, R. J.; Zhu, H.; Karakaya, C.; Chen, Y.; Ricote, S.; Jarry, A.; Crumlin, E. J.; Hook, D.; Braun, R. (2018). Highly durable, coking and sulfur tolerant, fuel-flexible protonic ceramic fuel cells. *Nature* *557*, 217-222.
146. Yu, Y.; Yu, L.; Shao, K.; Li, Y.; Maliutina, K.; Yuan, W.; Wu, Q.; Fan, L. (2020). $\text{BaZr}_{0.1}\text{Co}_{0.4}\text{Fe}_{0.4}\text{Y}_{0.1}\text{O}_3$ -SDC composite as quasi-symmetrical electrode for proton conducting solid oxide fuel cells. *Ceram Int.* *46*, 11811-11818.
147. Wang, Y.; Liu, T.; Fang, S.; Xiao, G.; Wang, H.; Chen, F. (2015). A novel clean and effective syngas production system based on partial oxidation of methane assisted solid oxide co-electrolysis process. *J. Power Sources* *277*, 261-267.
148. Liu, T.; Liu, H.; Zhang, X.; Lei, L.; Zhang, Y.; Yuan, Z.; Chen, F.; Wang, Y. (2019). A robust solid oxide electrolyzer for highly efficient electrochemical reforming of methane and steam. *J. Mater. Chem. A.* *7*, 13550-13558.
149. Zhu, C.; Hou, S.; Hu, X.; Lu, J.; Chen, F.; Xie, K. (2019). Electrochemical conversion of methane to ethylene in a solid oxide electrolyzer. *Nat. Commun.* *10*, 1-8.
150. Kyriakou, V.; Neagu, D.; Zafeiropoulos, G.; Sharma, R. K.; Tang, C.; Kousi, K.; Metcalfe, I. S.; van de Sanden, M. C.; Tsampas, M. N. (2020). Symmetrical Exsolution of Rh Nanoparticles in Solid Oxide Cells for Efficient Syngas Production from Greenhouse Gases. *ACS Catal.* *10*, 1278-1288.
151. Zhan, S.; Zhang, H.; Zhang, Y.; Shi, Q.; Li, Y.; Li, X. (2017). Efficient NH_3 -SCR removal of NO_x with highly ordered mesoporous $\text{WO}_3(\gamma)$ - CeO_2 at low temperatures. *Appl. Catal. B-Environ.* *203*, 199-209.
152. Liu, X.; Luo, Z.; Yu, C. (2019). Conversion of char-N into NO_x and N_2O

during combustion of biomass char. *Fuel* 242, 389-397.

153. Kim, Y. J.; Kwon, H. J.; Heo, I.; Nam, I.-S.; Cho, B. K.; Choung, J. W.; Cha, M.-S.; Yeo, G. K. (2012). Mn-Fe/ZSM5 as a low-temperature SCR catalyst to remove NO_x from diesel engine exhaust. *Appl. Catal. B-Environ.* 126, 9-21.

154. Cui, W.; Li, J.; Sun, Y.; Wang, H.; Jiang, G.; Lee, S.; Dong, F. (2018). Enhancing ROS generation and suppressing toxic intermediate production in photocatalytic NO oxidation on O/Ba co-functionalized amorphous carbon nitride. *Appl. Catal. B-Environ.* 237, 938-946.

155. Zarah Friedberg, A.; Kammer Hansen, K. (2017). NO_x and propene conversion in La_{0.85}Sr_{0.15}MnO_{3+δ}/Ce_{0.9}Gd_{0.1}O_{1.95} symmetrical cells. *J Electro. Sci. Engine* 7, 153-166.

156. Li, W.; Liu, X.; Yu, H.; Zhang, S.; Yu, H. (2020). La_{0.75}Sr_{0.25}Cr_{0.5}Mn_{0.5}O_{3-δ}-Ce_{0.8}Sm_{0.2}O_{1.9} as composite electrodes in symmetric solid electrolyte cells for electrochemical removal of nitric oxide. *Appl. Catal. B-Environ.* 264, 118533.

157. Shi, H.; Chu, G.; Tan, W.; Su, C. (2019). Electrochemical Performance of Ba_{0.5}Sr_{0.5}Co_{0.8}Fe_{0.2}O_{3-δ} in Symmetric Cells with Sm_{0.2}Ce_{0.8}O_{1.9} Electrolyte for Nitric Oxide Reduction Reaction. *Front Chem.* 7, 947-952.

158. Tong, Y.; Wang, Y.; Cui, C.; Wang, S.; Xie, B.; Peng, R.; Chen, C.; Zhan, Z. (2020). Preparation and characterization of symmetrical protonic ceramic fuel cells as electrochemical hydrogen pumps. *J. Power Sources* 457, 228036.

159. Minh, N. Q. (1993). Ceramic fuel cells. *J. Am. Ceram. Soc.* 76, 563-588.

160. Jung, D. W.; Lee, K. T.; Wachsman, E. D. (2014). Terbium and tungsten co-doped bismuth oxide electrolytes for low temperature solid oxide fuel cells. *J. Korean. Ceram. Soc.* 51, 260-264.

161. Jung, D. W.; Duncan, K. L.; Wachsman, E. D. (2010). Effect of total dopant concentration and dopant ratio on conductivity of (DyO_{1.5})_x-(WO₃)_y-(BiO_{1.5})_{1-x-y}. *Acta. Mater.* 58, 355-363.

162. Wachsman, E. D.; Lee, K. T. (2011). Lowering the temperature of solid oxide fuel cells. *Science* 334, 935-939.

163. Sanna, S.; Esposito, V.; Andreasen, J. W.; Hjelm, J.; Zhang, W.; Kasama, T.;

Simonsen, S. B.; Christensen, M.; Linderoth, S.; Pryds, N. (2015). Enhancement of the chemical stability in confined δ -Bi₂O₃. *Nat. Mater.* *14*, 500-504.

164. Hedayat, N.; Du, Y.; Ilkhani, H. (2018). Pyrolyzable pore-formers for the porous-electrode formation in solid oxide fuel cells: A review. *Ceram. Int.* *44*, 4561-4576.

165. Duan, N.; Yang, J.; Gao, M.; Luo, J. (2020). Multi-functionalities enabled fivefold applications of LaCo_{0.6}Ni_{0.4}O_{3- δ} in intermediate temperature symmetrical solid oxide fuel/electrolysis cells. *Nano Energy* *77*, 105207.

166. Othman, M H D.; Droushiotis, N.; Wu, Z.; Li, K. (2011). High-performance, anode-supported, microtubular SOFC prepared from single-step-fabricated, dual-layer hollow fibers. *Adv. Mater.* *23*, 2480-2483.

167. Kaur, G.; Kulkarni, A P.; Fini, D. (2020). High-performance composite cathode for electrolysis of CO₂ in tubular solid oxide electrolysis cells: A pathway for efficient CO₂ utilization. *J. CO₂ Util.* *41*, 101271.

168. Wang, Y.; Li, W.; Ma, L.; Li, W.; Liu, X. (2020). Degradation of solid oxide electrolysis cells: phenomena, mechanisms, and emerging mitigation strategies—a review. *J. Mater. Sci. Technol.* *55*, 35-55.

169. Xia, J.; Wang, C.; Wang, X. (2020). A perspective on DRT applications for the analysis of solid oxide cell electrodes. *Electrochim. Acta.* *349*, 136328.

170. Ren, B.; Li, J.; Wen, G. (2018). First-principles based microkinetic modeling of CO₂ reduction at the Ni/SDC cathode of a solid oxide electrolysis cell. *J. Phys. Chem. C.* *122*, 21151-21161.

171. Giuliano, A.; Nicollet, C.; Fourcade, S.; Mauvy, F.; Carpanese, M. P.; Grenier, J. C. (2017). Influence of the electrode/electrolyte interface structure on the performance of Pr_{0.8}Sr_{0.2}Fe_{0.7}Ni_{0.3}O_{3- δ} as Solid Oxide Fuel Cell cathode. *Electrochim. Acta.* *236*, 328-336.

172. Li, Y.; Li, Y.; Wan, Y.; Xie, Y.; Zhu, J.; Pan, H.; Xia, C. (2019). Perovskite oxyfluoride electrode enabling direct electrolyzing carbon dioxide with excellent electrochemical performances. *Adv. Energy. Mater.* *9*, 1803156.

173. Stangl, A.; Muñoz-Rojas, D.; Burriel, M. (2020). In situ and operando characterisation techniques for solid oxide electrochemical cells: Recent advances. *J Phys: Energy*. *3*, 012001.
174. Benck, J. D.; Rettenwander, D.; Jackson, A.; Young, D.; Chiang, Y. M. (2019). Apparatus for operando x-ray diffraction of fuel electrodes in high temperature solid oxide electrochemical cells. *Rev. Sci. Instrum.* *90*, 023910.
175. Tian, Y.; Liu, Y.; Naden, A.; Jia, L.; Xu, M.; Cui, W.; Chi, B.; Pu, J.; Irvine, J T S.; Li, J. (2020). Boosting CO₂ electrolysis performance: via calcium-oxide-looping combined with in situ exsolved Ni-Fe nanoparticles in a symmetrical solid oxide electrolysis cell. *J. Mater. Chem. A*. *8*, 14895-14899.
176. Zhu, C.; Hou, S.; Hu, X.; Lu, J.; Chen, F.; Xie, K. (2019). Electrochemical conversion of methane to ethylene in a solid oxide electrolyzer. *Nat. Commun.* *10*, 1-8.
177. Wang, H.; Kong, H.; Pu, Z.; Li, Y.; Hu, X. (2020). Feasibility of high efficient solar hydrogen generation system integrating photovoltaic cell/photon-enhanced thermionic emission and high-temperature electrolysis cell. *Energy. Convers. Manage.* *210*, 112699.
178. Cao, Y. (2020). A solar-driven lumped SOFC/SOEC system for electricity and hydrogen production: 3E analyses and a comparison of different multi-objective optimization algorithms. *J. Clean. Prod.* *271*, 122457.